Intra-tumoral injection of caerin 1.1 and 1.9 peptides in vaccinated TC-1 tumour bearing mice with PD-1 blockade modulates macrophage heterogeneity and the activation of $CD8^+$ T cells in the tumour microenvironment

Guoying Ni
First People's Hospital of Foshan
Xiaolian Wu
First People's Hospital of Foshan
Ying Liu
First People's Hospital of Foshan
Hejie Li
University of the Sunshine Coast
Shu Chen
First People's Hospital of Foshan
Conor Fogarty
University of the Sunshine Coast
Ian Frazer
University of Queensland https://orcid.org/0000-0002-8002-4680
Guoqiang Chen
First People's Hospital of Foshan
Xiaosong Liu
First People's Hospital of Foshan
Tianfang Wang (twang@usc.edu.au)
University of the Sunshine Coast https://orcid.org/0000-0002-4876-7767

Article

Keywords: tumors, tumor microenvironment, immunotherapy, vaccine formula

Posted Date: September 10th, 2020

DOI: https://doi.org/10.21203/rs.3.rs-73533/v1

Abstract

Development of a vaccine formula that alters the tumour-infiltrating lymphocytes to be more immune active against a tumour is key to the improvement of clinical responses to immunotherapy. Here, we demonstrate that, in conjunction with E7 antigen specific immunotherapy, and IL-10 and PD-1 blockade, intra-tumoral administration of caerin 1.1 and 1.9 peptides further improves the tumour microenvironment (TME) when compared with injection of a control peptide. We used single cell transcriptomics and mass spectrometry-based proteomics to quantify changes in cellular activity across different cell types within the TME. We show that the injection of caerin 1.1/1.9 increases immune activating macrophages and NK cells, while reducing immunosuppressive macrophages with M2 phenotype, and increased numbers of activated CD8+ T cells with higher populations of memory and effector-memory CD8+ T subsets. Proteomic profiling demonstrated activation of Stat1 modulated apoptosis and production of nitric oxide. Further, computational integration of the proteome with the single cell transcriptome was consistent with deactivation of immune suppressive B cell function following caerin 1.1 and 1.9 treatment.

Introduction

Human papilloma virus (HPV) infection accounted for 4.6% of 14 million new cancer cases reported worldwide in 2012, and HPV-associated cancers comprise 29.1% of all 2.2 million infection-related cancers, including nearly 100% of cervical cancers[1]. Cervical cancers are the 3rd most common cancer in women worldwide[2]. Moreover, high risk HPV infection, especially HPV16 infection, is related to a fraction of head and neck epithelial carcinoma in both developed and undeveloped countries[3]. HPV related cancers are most severe in developing countries where HPV prophylactic vaccination rates are low.

The use of immune checkpoint inhibitors has resulted in unprecedented rates of long-lasting tumour responses in patients with a variety of solid tumours[4]. However, immune checkpoint inhibitor monotherapy, such as PD-1[2] and CTLA-4 blockade[5] are less effective in the management of advanced cervical cancers[6]. PD-1 blockade combined with therapeutic vaccines synergise with each other to induce T cell-mediated tumour control, as animal models have demonstrated[7], including HPV16E6/7 transformed TC-1 tumour model[8]. Clinical trials also showed synergetic results of immune checkpoint blockade and therapeutic vaccination[9].

Cancer therapeutic vaccines aim at eliciting effector T cells, especially tumour antigen specific CD8$^+$ T cells that target tumour cells, without affecting the normal cells or tissues unaffected as demonstrated in clinical trials, such as those against melanoma[10]. However, vaccine-induced regression of high risk human papillomavirus infection related high-grade CIN lesions[11], but not established cervical cancers[12] were observed. Immunisation and simultaneous blocking of the cytokine interleukin 10 (IL-10) drastically increases vaccine induced antigen specific CD8$^+$ T cell responses and improved tumour growth inhibition in a prophylactic setting compared with the same vaccination without IL-10 signalling blockade[13].

Tumour inhibition was also improved in a therapeutic setting by intraperitoneal administration of anti-IL-10 receptor antibodies[14].

The immunosuppressive tumour microenvironment (TME) can dampen the function of tumour infiltrating effector T cells[15]. The TME promotes the development of tumour associated macrophages, myeloid derived suppressive cells, B cells, Th2 type T and regulatory T cells. Tumour associated macrophages (TAM) are attracting increasing attention as they play key roles in tumour spread and in response to different therapies[16]. TAM can substantially accelerate the progression of untreated tumours, but also influence the efficacy of anticancer drugs, including checkpoint blockade immunotherapies[17, 18]. Specifically, TAM can assume opposing phenotypes and functions that are either tumoricidal (e.g., M1-like MΦ) or tumour-supportive (e.g., M2-like MΦ).

Host-defence caerin peptides isolated from Australian amphibians, *Litoria genus*, were observed to be active against cancer cells, such as TC-1[19], HeLa[20, 21]. Caerin 1.1 and 1.9 inhibit HIV-infected T cells within minutes post-exposure at concentrations non-toxic to T cells, and inhibit the transfer of HIV from dendritic cells (DCs) to T cells[22]. They are cytotoxic to HPV18+ HeLa cells, and HPV 16 early protein E6/E7 transformed TC-1 cells *in vitro*, and the anti-tumour effects were more profound when caerin 1.1 and 1.9 were used together[19]. Moreover, caerin1.1 and 1.9 were able to inhibit TC-1 growth *in vivo* when locally injected intratumorally, and the inhibition requires an intact adaptive immune system[13, 20]. The signalling of TNFα mediated apoptosis and T-cell receptor was stimulated after HeLa cells were treated with the mixture of caerin 1.1 and 1.9[21]. Activation of TCR pathway observed in proteomic analysis suggested that HeLa cells became more sensitive to T cell mediated killing[21].

In this study, TC-1 tumour bearing mice immunised with a HPV16 E7 peptide-based vaccine containing anti-IL-10 receptor antibody and PD-1 blockade were locally injected with a mixture of caerin 1.1 and 1.9 peptides. Tumour-infiltrating lymphocytes (TILs) were isolated for scRNA-seq analysis to reveal the cell types of TILs in TC-1 tumour and the modulation of the TIL landscape by the immunotherapy containing caerin 1.1/1.9. Mass spectrometry-driven quantitative proteomic analysis was performed to investigate the overall effect of the changes in TILs. Our study provides new insights into the heterogeneity of TILs and their functions in TC-1 tumour, including novel markers to define immune activating macrophages and $CD8^+$ T cell subpopulations, as well as the molecular mechanisms underlying TME modulation by caerin 1.1/1.9.

Results

Single cell RNA-seq identified six different macrophage populations in TC-1 tumour

In this study, untreated TC-1 tumour bearing mice and tumour bearing mice immunised with a HPV16 E7 peptide-based vaccine containing anti-IL-10 receptor antibody and PD-1 blockade were locally injected with a mixture of caerin 1.1 and 1.9 peptides (molar ratio 1:1) (“caerin”) or a control peptide. The two treatment groups showed significantly reduced tumour mass when compared with the untreated group,

with a reduction of 69% (caerin, *P*=0.0011) and 42% (control peptide, *P*=0.0352). An additional injection of caerin further reduced the tumour weights, though the reduction was insignificant (*P*=0.11). Elispot results from spleen and draining lymph nodes (LN) of individual mice (3 mice) indicate that two immunotherapy and peptide treated groups demonstrated similar E7 specific $CD8^+$ T cells in the spleen and draining lymph nodes (**Fig. 1A**).

Thirty days after TC-1 tumour challenge, total viable $CD45^+$ leukocytes were isolated from tumours using a tumour infiltrating cell isolation kit (**Fig. 1B** and **Supplementary Data 1**). Gene expression data from cells extracted from the control tumours and the two treated tumours were aligned and projected in a 2-dimensional space through t-stochastic neighbour embedding (t-SNE) to allow identification of tumour associated immune cell populations and the overlapping patterns associated with the control tumours and the two treated tumour groups (**Fig. 1C** and **Supplementary Fig. 1**). There were 19 distinct cell clusters (Cluster 0 to 18) detected by using unsupervised graph-based clustering method (see Methods) (**Fig. 1C** through **1E; Supplementary Fig. 2A** to **2D**). The presence of lymphocyte lineages was supported by the established canonical markers, such as *Nkg7*, *Cd19*, *Fcmr*, *Cd8b1* and *Cd79a*, as well as myeloid cells that were determined by the identifications of *Cd11c*, *Cd14*, *Cd68*, *Cd209a, Adgre1*, *Itgax, Csf1r*, *Lgals3*, *Ccr2* and *Ly6c2*[23, 24]. The populations and expression patterns of a few marker genes were shown in **Fig. 1D** and **1E** (see **Supplementary Data 2** for the full list of all marker genes detected).

Nonmacrophage cell populations were identified as monocytes (cluster 0; marker genes: *Ly6a*, *Ly6c2*, *Fcgr1* and *Dpep2*), neutrophils (cluster 7; *Retnlg*, *S100a8*, *Cxcl2*, and *Hdc*), B cells (cluster 11; *Cd79a*, *Fcmr*, *Ly6d*, and *Mzb1*), conventional DC type 2 (cDC2) (cluster 12; *Cd209a*, *Flt3*, *Ctnnd2*, and *Epcam*)[25], natural killer (NK) cells (cluster 14; *Gzma*, *Xcl1, Ncr1*, and *Klrb1c*), migratory DCs (migDC) (cluster 16; *Ccl22*, *Bcl2l14*, *Fscn1*, and *Cacnb3*)[26], plasmacytoid dendritic cells (pDCs) (cluster 18; *D13Ertd608e*, *Siglech*, *Ccr9*, and *Pacsin1*)[25] and four clusters with gene signatures suggesting various phenotypes of T cells (clusters 5, 10, 13 and15). Fibroblast (cluster 4; *2810417H13Rik*, *Tk1*, *Birc5*, and *Cdca3*), adipogenic stem and precursor cells (ASPCs) (cluster 6; *Gas1*, *Igfbp3*, *Col3a1*, *Mgp* and *Cyr61*)[27] were also identified as contaminants (also see **Supplementary Data 2** and **Supplementary File 1**).

The macrophage populations were examined in more detail, and expression of the top 20 marker genes of each macrophage population was compared to their expression across all macrophage cell populations, and to the expression of other genes in the same macrophage population (**Fig. 1F**). Specific gene expression patterns differentiating these MΦ populations and certain overlaps could be determined. Many of the top 20 marker genes of cluster 1, including *Pf4*, *Arg1*, *Fabp5*, and *Mmp12*, were associated with M2 MΦ (**Fig. 1F**; **Supplementary Data 2**), and similar numbers of these cells were detected in tumours treated with caerin peptides or control peptide. (**Supplementary Fig. 2C** and **2D**). The top three highly expressed genes with significance in cluster 2 were *H2-Eb1*, *Cd74* and *C1qc* (**Supplementary Data 2** and **Supplementary File 1**), confirming a MΦ signature. These genes were found to mark $MHCII^{hi}$ border associated MΦ in mouse brain[26]. The high expressions of several H-2 (*MHCII*) members, including *H2-Eb1*, *H2-Ab1*, *H2-Aa*, *H2-DMb1* and *H2-DMa*, were also confirmed in cluster 2, thus we considered these as

MHCII^{hi} MΦ hereafter. Cluster 3 had a mixed cell phenotype, including proinflammatory MΦ (*Cxcl10*, *Gbp2*, and *Thbs1*), *Ly6c*^{hi} infiltrating MΦ (*Chil3* and *Plac8*), and dendritic cells (*Rsad2*, *Ifit1*, *Ifit2* and *Ifi205*). Thus, this cluster was labelled as MΦ/DCs. Increase in the size of this cluster in caerin peptide and control peptide treated tumours suggested that analysis of its subpopulations might help to further clarify its function. It was mainly composed of macrophages (*Nop16*, *Gatm* and *Pf4*) and NKT cells (*Ntpcr*, *Mrpl28* and *Commd10*), and was identified as MΦ/NKT. Due to the exclusive high expression of *Ear2* in cluster 9, it was assigned as *Ear2*^{hi} MΦ (*Chil3*, *Adgre5*, *Ace*, and *Ifitm6*)[28, 29]. Cluster 17 exhibited the signatures of MΦ (*Adgre1*, *Csf1r*, *Fcgr1*, and *Cd68*) and there was upregulated chemokine gene expression (*Ccl8*, *Ccl24*, *Ccl6*, and *Ccl9*) (**Supplementary Data 2** and **Supplementary File 1**), suggesting that these might be tumour associated MΦ (TAM) as *Ccl8* and *Siglec1* are markers for TAMs in breast cancer[30], and both were highly expressed in this cluster, with *Ccl8* expression exclusive to cluster 17 (**Supplementary Data 2**). The presence of other significantly upregulated genes, e.g., *Cd209f*, *Clec10a* and *Cd163*, also indicated the existence of activated M2 MΦ. Thus, we consider cluster 17 as TAMs. In comparison to other clusters, the top 20 marker genes of cluster 8 appeared less significant as indicated by their relatively higher *P*-values (*P*>1.0E-34) (**Supplementary Data 2**).

We found that, in comparison to the untreated tumours, the tumours from the two immunised and peptide treated groups had significantly increased populations of monocytes, *MHCII*^{hi} MΦ, MΦ/DCs, *Ear2*^{hi} MΦ, CD8^{+} T cells, and pDCs and substantially reduced M2 MΦ and B cell populations (**Supplementary Data 1**; **Supplementary Fig. 2C** and **Fig. 2D**). CD8^{+} T cells appeared nearly exclusive to tumours from immunised animals, and the M2 MΦ population was reduced in these tumours, possibly due to the use of anti-IL10 antibody in the immunisation, since it directly associates with the secretion of IL10[31]. Numbers of *MHCII*^{hi} MΦ and NK cells were greatest in caerin peptide treated tumours. Notably, B cells were almost depleted from tumours treated with caerin peptide (15/5,685 cells), when compared to tumours from untreated animals (194/4,011 cells) and control peptide and immunisation treated animals (87/5,415 cells) (**Supplementary Data 1**).

Intratumor injection of caerin peptides significantly increased *Arg1*$^{-}$ tumour infiltrating macrophages

Six macrophage populations were detected, including M2 MΦ, *MHCII*^{hi} MΦ, MΦ/DCs, *Ear2*^{hi} MΦ, MΦ/NKT and TAMs. Altogether, these macrophages represented the largest cell populations (**Supplementary Fig. 3**), constituting 49.58% of total cells in the untreated TC-1 tumour, and a similar fraction of total cells in immunised animals treated with caerin peptide (47.47%) or control peptide (42.00%) (**Supplementary Data 2**). The correlation between each group of MΦs were derived based on the expression of significantly upregulated genes (**Fig. 2A**). Notably, M2 MΦ and *MHCII*^{hi} MΦ were highly correlated with MΦ/NKT, suggesting close development of these MΦ lineages. The normalised numbers of different MΦs in the tumours were compared between the control and treated animals, and M2 MΦ were reduced in tumours in the immunised and peptide treated animals by about 80% (**Fig. 2B**). Injection of caerin largely induced *MHCII*^{hi} and *Ear2*^{hi} MΦs in tumours, while reducing TAMs, when compared to tumours from untreated animals or receiving control peptide treatment. M2 MΦ was reduced from 73.2% of

macrophages in untreated tumour to 16.2% in caerin and 18.9% in control peptide treated tumours (**Fig. 2C**). In contrast, the proportions of *MHCII*^{hi} MΦ were elevated by approximately 5-fold (caerin peptide) and 4-fold (control peptide) treated tumours, and MΦ/DCs and *Ear2*^{hi} MΦ were similarly increased in the caerin and control peptide treated tumours.

We next sought to unravel the phenotype and functions behind the specific gene expression patterns of each macrophage. The expressions of key lineage-associated genes of M2 MΦ were compared in parallel with their expressions in other macrophages (**Fig. 2D**). Several marker genes appeared exclusive to M2 MΦ, such as *Mmp12*, *Arg1*, *Mmp13* and *Slc6a8*, for which expression is associated with tumour angiogenesis and invasiveness[32, 33, 34]. The role of *Arg1* in immunosuppression has been described elsewhere[35]. Some marker genes of M2 MΦ were also highly expressed in TAMs, suggesting potential similarity between these two macrophages in terms of cellular function.

The distribution of M2 MΦ in untreated tumours and tumours injected with caerin peptides was compared in **Fig. 2E**. The expression of some marker genes (*Rcgg*, *Ndrg1* and *Egln3)*, aligned well with those of M2 MΦ after peptide treatment. The relative expression of the top 40 marker genes of M2 MΦ were hierarchically clustered and compared amongst untreated and peptide treated tumours (**Fig. 2F**). All genes were significantly downregulated in caerin and control peptide treated tumours, except *Mmp13* in the control peptide treated tumours and *Ndrg1* in the caerin treated tumours. To evaluate the significance of this observation, the expression values of selected genes were further compared, where significant downregulation of *Arg1*, *Mmp13*, *Pf4* and *Hmox1* were present in caerin treated tumours when compared to control peptide treated tumours (**Fig. 2G**). Most of the biological processes enriched in M2 MΦ represented by the marker genes unique to caerin treated tumours related to immune responses including apoptosis, responses to stimulus with organic substance, cytokine production and secretion, and T cell differentiation (**Fig. 2H**). Different gene expression patterns relating to metabolism and transport of macromolecules (**Supplementary Fig. 4B**), and responses to heat and wounding (**Supplementary Fig. 4C**) were found in the untreated tumours and those treated with control peptide.

MHCII^{hi} MΦ were significantly increased in control and caerin peptide treated tumours, more significantly with caerin treatment. The expression of selected marker genes across six macrophage populations were displayed in **Fig. 3A**, which suggests *Lira5*, *Cxcl9*, *Dnase1l3* and *Cd300e* as the signatures exclusive to *MHCII*^{hi} MΦ. *Cadm1*, *Cxcl9* and *Cd300e* expression was increased in macrophages, and *Dnase1l3* has been reported as a signature of CD141^{+}CLEC9A^{+} DCs[36]. In addition, *Clec12a* was recently found to highly expressed in myeloid cells including macrophages and DC subsets[37]. Thus, the *MHCII*^{hi} MΦ cluster displayed a characteristic of mixing phenotypes and its subpopulations were further investigated.

A total of five subpopulations of *MHCII*^{hi} MΦ were identified and projected in a 2-dimensional tSNE space, with the subpopulation 0, 1 and 2 possessing the highest cell numbers (**Fig. 3B**). Subpopulation 3 was present in control and caerin peptide treated tumours in similar numbers, while subpopulation 4 was negligible in untreated tumours (**Supplementary Data 3**). The normalised cell numbers of five

subpopulations with different treatments were compared in **Fig. 3C**, and caerin peptide treatment stimulated much higher number of subpopulations 0, 1 and 2 when compared to control peptide treatment (group C), with fold changes of 4.22, 8.14 and 3.89 relative to the untreated group. The expressions (Log2 FC) of the top 10 marker genes of each subpopulation were compared across all five subpopulations (**Fig. 3D**). The first subpopulation, C0_*MHCII*^{hi}-CXCL2, characterised by *Cxcl2*, *Nfil3* and *Osm*, had the phenotype of activated macrophages[38, 39, 40]. The second subpopulation showed significant expressions of *Ifit3b*, *Ifit3* and *Ifit2*, typical of polarised M1 macrophages[41], suggesting pro-inflammatory function. In addition, this subpopulation also showed significant upregulation of several other interferon-induced protein relevant genes, thus we labelled it as C1_*MHCII*^{hi}-IFIT.

The third subpopulation had the lowest number of significantly upregulated genes compared to other four subpopulations, and was characterised by expression of *Fcrls*, *Ptgs1*, *Mrc1* and *Igfbp4,* the signature of resident-like macrophages[26, 42, 43]. Thus, this subpopulation is referred as C2_*MHCII*^{hi}-ResMΦ. The fourth subpopulation, named C3_*MHCII*^{hi}-DCs, possessed the highest number of marker genes and the top marker genes, including *Ankrd33b*, *Xrc1*, and *Asb2* were typical of DCs. Also, the signature gene of B cells, *Fcrl5*, was significantly expressed in C3_*MHCII*^{hi}-DCs, suggesting antigen presentation capacity. The fifth subpopulation was characterised by several marker genes of progenitor cells, such as *Birc5*[44], *Cdkn3*[45], *Ccnb2*[46] and *Kif20a*[47], which was referred as C4_*MHCII*^{hi}-PROG. The H-2 (MHCII) members were mainly elevated in C1_*MHCII*^{hi}-IFIT and C4_*MHCII*^{hi}-PROG.

The correlations amongst these subpopulations were evaluated based on the upregulated genes (**Fig. 3E**). C1_*MHCII*^{hi}-IFIT and C3_*MHCII*^{hi}-DCs were correlated to a much higher degree, compared to the connections amongst other three clusters. Genes that were shared between C1_*MHCII*^{hi}-IFIT and C3_*MHCII*^{hi}-DCs revealed biological processes mutually exerted by these two subpopulations, including metabolism of lipids and lipoproteins, G-protein signalling and FCGR activation. Reactome pathways based on marker genes that were unique to each subpopulation were analysed (**Supplementary Fig. 5**). C0_*MHCII*^{hi}-CXCL2 showed an enrichment in caspase-mediated cleavage of cytoskeletal proteins, immune system, apoptotic cleavage of cellular proteins and apoptotic execution phase. The signalling of interferon, interferon gamma and cytokine in immune system were detected in C1_*MHCII*^{hi}-IFIT with significance. The pathways found in C2_*MHCII*^{hi}-ResMΦ were less significant (high *P*-values) than those in other subpopulations, such as GPCR ligand binding, chemokine receptors bind chemokines and collagen formation, which were less relevant to activating immune response. C3_*MHCII*^{hi}-DCs showed enrichment in haemostasis, GPVI-mediated activation cascade and adaptive immune system. Many cell cycle related pathways were found enriched in C4_*MHCII*^{hi}-PROG (**Supplementary Data 3**).

The populations of *Ear2*^{hi} MΦ were remarkably elevated in control peptide and particularly in caerin peptide treated tumours (**Supplementary Fig. 6A**). The distribution of cells expressing selected pro-inflammatory marker genes appeared aligned well with *Ear2*^{hi} MΦ in caerin peptide compared to untreated and control peptide treated tumours. Significant upregulation of *Ear2*, *Ace*, *Adgre4*, *Serpinb2*

and *Prtn3* in *Ear2*^{hi} MΦ was identified in the caerin treated tumours compared to untreated tumours (**Supplementary Fig. 6B**). A High degree of gene expression concordance c was present amongst *Ear2*^{hi} MΦs, yet distinct biological processes were found in subgroups *Ear2*^{hi} MΦ (**Supplementary Fig. 6C**). *Ear2*^{hi} MΦ showed the suppression of many biological processes, such as transferase activity, phosphorylation, and cellular protein metabolism in untreated tumours, when compared to the activation of metabolic processes in control peptide treated tumours. Caerin treated tumours had activated cellular structure remodelling and immune response genes including those suggesting myeloid cell differentiation.

More CD8$^+$ T cells infiltrate to TC-1 tumour following vaccination and PD-1 blockade, and CD8$^+$ T cells are more activated in caerin 1.1/1.9 treatment group B

In control peptide and caerin peptide treated tumours, the population of CD8$^+$ T cells infiltrating to TC-1 tumour was was 3.73% (caerin) and 4.58% (control peptide) of the total CD45$^+$ cells compared to only 0.27% in untreated tumours (**Supplementary Data 1**). With peptide treatment, CD8$^+$ T cells were relatively separated from other three T cell populations on the tSNE graph (**Fig. 4A**), indicating a possible variation in function. Also, all T cell types showed a more than 10-fold increase between untreated tumours to 40% (caerin) and 37% (control peptide) (**Fig. 4B**). Analysis of the gene expression pattern in the four T cell populations (**Fig. 4C**.) showed that expression of most of these genes was higher in CD8 T cells than that in any other T cell type (see **Supplementary Fig. 5** for the expression of marker genes in other T cells), including genes that enhance the activation of CD8$^+$ T cells, such as *Ucp2*, *Fth1*, *Apoe*, *Fcer1g* and *Calm3*.

Since pDCs present antigens (Ag) and induce immunogenic T cell responses through differentiation of cytotoxic CD8$^+$ T cells and effector CD4$^+$ T cells[48, 49], we compared the gene expression of signature genes of CD8$^+$ T cells across four types of T cells and pDCs (**Fig. 4D**). It shows that *Cd8a*, *Klrc1* and *Lag3* were almost exclusive to CD8$^+$ T cells, while comparable expression of *Cxcr6* was observed in CD4$^-$CD8$^-$ T cells, and lower expression of *Cd8a*, *Cd8b1* and *Lag3* was observed in pDCs. Ribosome was determined to be the most enriched KEGG pathway, followed by T cell receptor signalling and natural killer cell mediated cytotoxicity (**Fig. 4E**). The top 25 enriched biological processes in CD4$^+$CD8$^+$, CD8$^+$, CD4$^+$CD25$^+$ and CD4$^-$CD8$^-$ T cells were compared in **Fig. 4F**. Translation was found to be the most enriched process in the T cell subsets except CD4$^+$CD25$^+$, and was subsequently excluded to highlight the difference amongst other enriched processes (**Supplementary Data 5**). Since these cells share similar T cell lineage development, overlaps of certain biological processes were observed, such as T cell differentiation, T cell receptor signalling, and innate immune response was observed as expected. However, T cell relevant processes were more enriched in CD8+ T cells suggested by lower *P*-values compared to other three subtypes. Furthermore, there were a set of processes only enriched in CD8$^+$ T cells, such as positive regulation of histone deacetylation, regulation of translational initiation, chromosome organisation, activation of cysteine-type endopeptidase activity involved in apoptotic process and regulation of cytokine production (**Fig. 4F** and **Supplementary Data 5**).

The expression of marker genes, including *Cd8a*, *Cd8b1*, *Tox*, *Lag3*, *Ifng*, *Nkg7*, *Nrgn*, Gldc, *Prf1*, *Abcb9*, *Nrn1* and *Rgs16*, were compared amongst untreated, caerin, and control peptide treated tumours (**Fig. 5A**), where significant upregulations of these genes induced by peptide treatment were observed, except *Nrn1* for the control peptide treatment. In addition, *Cd8a*, *Cd8b1*, *Tox*, *Ifng*, *Prf1* and *Rgs16* were significantly elevated by caerin when compared to control peptide, suggesting that $CD8^+$ T cells were more activated by the caerin peptide. The subpopulations of $CD8^+$ T cells were further investigated to reveal the changes of heterogeneity due to peptide treatment, and five subpopulations were identified (**Fig. 5B**; **Supplementary Fig. 8**). We found that the signatures representing naïve T cells, including *Sell*, *Lef1* and *Tcf7*, had higher expression in untreated tumour (**Fig. 5C**). Peptide treatment caused elevation of signatures for exhausted T cells, such as *Tigit*, *Lag3*, *Tox* and *Pdcd1*, while the effector T cells were stimulated by two treatments, suggested by the upregulation of *Gzmb* and *Prf1*. The expression of these genes in the five CD8 subpopulations was also compared to reveal their possible functions. The average expression of the top 20 markers genes of five subpopulations were compared in **Supplementary Fig. 8E**, where the marker genes of subpopulation 2 and 3 were more exclusive.

The first cluster C0_CD8-CCL5 cells characterised by marker genes *Ccl5*[50], *Cd3e*[51], *Cxcr6*[52] and *Gzmk*[53], were considered as memory T cells. Most of the top 20 highly expressed genes in the second cluster were various ribosomal proteins, such as *Rpl32*, *Rpl26*, *Rpl23* and *Rpl28*. It has been reported that translation is upregulated during effector $CD8^+$ T cell expansion[54]. In addition, *Tnfrsf9*[55] and *Prf1*[56] appeared to highly express in this subpopulation. Thus, these were likely effector $CD8^+$ T cells and were named C1_CD8-TNFRSF9. The third cluster, C2_CD8-CDCA5, was characterised by significant upregulation of *Cdca5*, *Cdc6* and *Ccna2* (**Supplementary Data 5**), commonly associated with dividing T cells[57]. Additionally, several histones and regulators, including *Tmsb10* and *Ptma*, were among those genes with highest expression in C2_CD8-CDCA5. The fourth cluster possessed more than 1,500 genes with significant upregulation (**Supplementary Fig. 8**) and was characterised by *Fth1*, *Cd74*, and *Ifitm3*. The relevance of *Fth1* to $CD8^+$ effector T cell response was reported, which revealed that it played an immunomodulatory role in cytokine signalling, adaptive immunity, and cell death[58]. The high expression of *Cd74* and *Ifitm3* was detected in memory T cell[53, 59]. Thus, this cluster was comprised of effector-memory T cells, referred as C3_CD8-FTH1 hereafter. The remaining cell cluster, C4_CD8-MS4A4B, was characterised by *MS4a4B*, *Ly6a*, *Cd8b1*, *Ly6e*, and were naïve T cells. Notably, the $CD8^+$ T cells of untreated tumours only contained two of five subpopulations, i.e., C0_CD8-CCL5 and C2_CD8-CDCA5, while the control peptide and caerin peptides induced all five subpopulations (**Fig. 5B**; **Supplementary Fig. 8A**; **Supplementary Data 5**). Caerin treated tumours possessed higher number of C0_CD8-CCL5 and C3_CD8-FTH1 compared to the control peptide treated tumours.

We then projected $CD8^+$ T cells onto the two-dimensional state-space defined by Monocle3 for sample similarity and pseudotime analysis, to obtain the information inferring

lineage trajectories from expression data (**Fig. 5C**). Most cells from each subpopulation aggregated based on expression similarities, and different clusters formed into a relative process in pseudotime that

began with C2_CD8-CDCA5 (dividing $CD8^+$ T cells), then developed in separate directions, with one direction developing to C3_CD8-FTH1 cells (effector-memory $CD8^+$ T cells). It appeared that C0_CD8-CCL5 (memory $CD8^+$ T cells), C1_CD8-TNFRSF9 (effector $CD8^+$ T cells) and C4_CD8-MS4A4B (naïve $CD8^+$ T cells) started to emerge at approximately similar pseudotime on the other direction, gradually overlapping on three branches along the pseudotime trajectory, two of which also included certain amount of C2_CD8-CDCA5 cells, indicating functional divergence of this subpopulation. On these two branches, C2_CD8-CDCA5 aggregated with C0_CD8-CCL5 and C1_CD8-TNFRSF9, which suggested close correlation between regulatory, effector and memory $CD8^+$ T cells, and different functions might be executed. C4_CD8- MS4A4B was diversely present together with C0_CD8-CCL5 and C1_CD8-TNFRSF9 along the pseudotime, especially at the middle area (**Fig. 5C**), implying their close association.

Seven states were thus identified based on pseudotime analysis (**Fig. 5D**), where cells in transitional state 2 and state 5 exclusively corresponded to C0_CD8-CCL5 and C2_CD8-CDCA5, respectively. Most cells of state 1, 3 and 7 were C0_CD8-CCL5, C1_CD8-TNFRSF9 and C2_CD8-CDCA5. A transitional state 4 was identified, which consisted of all clusters except C3_CD8-FTH1. The predicted developmental trajectory was also confirmed by the marker genes with similar expression pattern, which hierarchically clustered these markers along the pseudotime in each state (**Supplementary Fig. 8**). States 1, 6 and 7 included genes with expression gradually increasing with the time. The potential divergence of cell functions in different state cells were investigated (**Supplementary Data 5**). Notably, state 1 showing significantly elevation of genes enriched in the signalling pathways of IL-2 and IL-3, G protein, and G13 at a later stage, and caerin treated tumours had a higher population in this state compared to untreated and control peptide treated tumours (**Fig. 5D** and **Supplementary Data 5**). Apoptosis was the only pathway enriched in state 3, and signalling by EGFR1, chemokine and TGF-β was present in state 7. The transition state 2 between state 3 and 7 had very different functions, such as the enrichments of macrophage markers, ApoE and miR-146 in inflammation and atherosclerosis, and antigen processing and presentation. The presence of more state 6 cells at late pseudotime potentially associated with caerin treatment correlated with the marker genes playing roles in TNFα, NF-kB signalling and inflammatory response.

The genes significantly differentiating the branches were also analysed, with expression variation of top 10 genes along the pseudotime trajectory compared amongst different groups (**Fig. 5F** to **5H**). Most of these genes were expressed around pseudotime zero in the untreated tumours but had a significantly prolonged expression with control or caerin peptide treatment. During the first transition, the genes highly associated with immune system, and their expression, declined at an early stage in states 5 and 6 possibly due to low cell numbers, then increased sharply onwards pseudotime 25, where more cells expressing these genes were observed in caerin treated tumours. There was also a slow increase of expression of *Apoe*, *C1qb*, *Cd74*, *H2-Aa*, *H2-Ab1*and *H2-Eb1* along the pseudotime on the branch involving state 1, 2, 3, 4, 5 and 7, which also correlated with higher cell number stimulated by caerin (**Fig. 5F**). Most of genes such as *Rps11*, *15a*, *36*, *24* and *26* during the branching displayed in **Fig. 5G** appeared downregulated along the pseudotime in state 1, 2, 4 and 5, indicating the deactivation of translation, which was also the case in state 1, 2, 4, 5 and 7 for the third trajectory separation (**Fig. 5H**). In addition,

the expression trend of these genes in state 3, 4 and 5 aligned well with the cell distribution in caerin treated tumours.

TMT10plex labelling quantitative proteomics revealed higher immune response induced by the injection of caerin 1.1/1.9

To validate our scRNA-seq data and capture treatment-dependent alterations in protein content for the TC-1 tumour, we performed quantitative proteomic analysis of tumours using the TMT labelling method (details of protein quantitation and annotations are in **Table S6**). The pairwise comparison showed that significantly more proteins were regulated with caerin treatment when compared to control peptide (**Supplementary Fig. 9A** and **9B**). The hierarchical clustering of quantified proteins implied consistency between biological triplicates of each group. A total of 238 proteins were uniquely upregulated in with caerin treatment, while the upregulation of 51 proteins were observed with both caerin and control peptide treatments (**Supplementary Fig. 9C**).

The gene ontology (biological process, molecular function, and cellular component) enrichment of upregulated proteins with each treatment was carried out (**Supplementary Data 6**; **Supplementary Fig. 10**; **Supplementary Fig. 11**). With caerin, the enrichment of many biological processes was more significant than with control peptide, including immune system process (FDR=8.10E-28 with caerin versus 1.29E-12 with control peptide), and innate immune response (caerin, FDR=9.85E-22; control, FDR=3.60E-05). The top 60 proteins significantly regulated by caerin were shown in **Fig. 6A**. Caerin induced significant upregulation of proteins involved in immune response and regulation processes, such as *Gzma*, *Gzmc*, *Irf5*, *Tgtp1*, *Prg2* and *Ighg1*. The quantities of selected proteins uniquely regulated by caerin is shown in **Fig. 6B**.

The protein-protein interaction (PPI) analysis of upregulated proteins identified intensive interactions in both treatments (**Fig. 6C** and **6D**; the complete predicted PPIs were recorded in **Supplementary Data 6**; the statistical analysis of PPIs was presented in **Supplementary File 2**). Similar nodes can be found on two networks with different interaction degrees, with *Stat1* being the node with highest degrees with caerin and *B2m* with control peptide treatment. The fold changes of top 10 most interacting protein nodes on two PPIs were compared with respect to internal references (**Fig. 6E**). Most of these proteins showed higher contents with caerin than with control peptide. *Stat1* was upregulated by 2.2-fold compared to untreated tumour (**Supplementary Data 6**) and detected as a marker gene only in monocytes, MΦ/DCs and $CD4^+CD25^+$ T cells with caerin treatment (**Supplementary Data 6**) with no significant change in protein or mRNA with control peptide treatment.

The top 40 enriched biological processes were compared in **Fig. 6F**. Caerin treatment caused significant upregulation of proteins involved in immune response and regulation processes in the tumour, while many proteins upregulated appeared to play important roles in the processes related to antigen processing and presentation following control peptide treatment. This correlated with the finding that the injection of caerin largely reduced the population of B cells as suggested by the scRNA-seq

(**Supplementary File 2**). A correlation was observed between proteins significantly upregulated only with the injection of caerin and cell populations identified in scRNA-seq (**Fig. 6G**). Of those proteins showing a fold change greater than 2, many were closely correlated with normalised expressions of genes in the populations of monocytes, MΦ and DCs, such as *Iigp1*, *Gbp2*, *Irf5* and *Parvg*. There were a few proteins more closely associated with their gene expression in T cell and NK populations, including *Satb1*, *Spn*, *Dok2* and *Hip1r*. Marker gene *Gzmc* appeared exclusive to NK cells, and protein upregulation was only considered significant with injection of caerin. *Stat1* was detected as an upregulated gene in nearly all cell populations except B cells and was elevated with caerin treatment in the proteomic analysis, suggesting that *Stat1* was largely regulated by caerin.

The KEGG pathways enriched (*P*-value<0.05) in upregulated proteins were compared for the different treatment in **Fig. 6H**, and more pathways were significantly identified with the caerin treatment, including apoptosis, natural killer cell mediated cytotoxicity, necroptosis, the signalling of nod-like receptor (NLR), TNF, chemokine, NF-Kappa B, RIG-I like receptor and toll-like receptor and several disease-related pathways. Amongst these KEGG pathways, NLR signalling was determined as the most enriched pathway (*P*-value=1.55E-10), supported by the significantly increased concentrations of *Gbp2*, *Gbp5*, *Nlrc4, Ccl2, Tlr4* and so forth by caerin treatment; the genes of many of these proteins were detected as signatures for MΦ/DCs by scRNA-seq. Notably, the antigen processing and presenting KEGG pathway was less significantly changed with caerin treatment (*P*-value=6.0E-4) compared to control peptide treatment (*P*-value=1.0E-11), in accordance with the observation that the population of B cells was remarkably reduced by the injection of caerin peptides.

Discussion

Here, we demonstrated that intra-tumour injection of caerin 1.1/1.9 peptides further modulated the TME in TC-1 tumour bearing mice immunised with a HPV16 E7 peptide based therapeutic vaccine coupled with PD-1 blockade, when compared with intra-tumour injection of a control peptide. The scRNA-seq of $CD45^+$ tumour infiltrating cells and proteomic analysis of tumour uncovered that caerin 1.1/1.9 changed heterogeneity and function of tumour infiltrating leukocytes, especially macrophage populations (largely elevated the populations of Arg^-, $MHCII^{hi}$ and $Ear2^{hi}$ MΦs), reducing pro-tumorigenic B cells and inducing more active $CD8^+$ T cells, which thus modulated the TME to a pro-inflammatory environment that may favour tumour rejection.

The numbers of tumour infiltrating $CD8^+$ T cells are similar between the treatment groups (**Fig.4**), but significantly more than those of untreated group. Although the antigen specific $CD8^+$ T cells in the spleen and draining lymph nodes are similar in the two treatments, suggesting that caerin peptides do not influence the generation of vaccine induced $CD8^+$ T cells (**Fig. 1A**), the $CD8^+$ T cells in caerin 1.1/1.9 group were more activated than those isolated from control group, with *Ifng, Pfr1, Rgs16* highly expressed in the former. We are currently investigating whether the improved TME by caerin1.1/1.9 treatment can be

translated to increased survival time in this group, together with therapeutic immunisation and PD-1 blockade.

Most of our knowledge of TAMs comes from histological examinations and *in vitro* profiling using flow cytometry[60]. There remains a significant knowledge gap on how TAMs function *in vivo* and how these cellular activities can be harnessed to improve anticancer therapy. Recently, it have been shown that macrophages, as well as other tumour infiltrating cells, have heterogeneous phenotypes in the tumour microenvironment by single cell RNA sequencing technology[61]. Similar results were observed here that six populations with distinct gene expression patterns and opposing functions were identified (**Figs. 2** and **3**). The immunosuppressive TAM phenotype ("M2") is generally believed to be positive for *Arg1*[62], due to the production of interleukin-4 and lactic acid by tumour cells. The M2 MΦ were abundant in untreated group, while the treatment groups displayed a substantial reduction in this type of MΦ. Furthermore, *Arg* expression in macrophage was significantly reduced by caerin 1.1/1.9 treatment, so were *Pf4*, *Mmp13* and *Hmox1*, known to promote tumorigenesis and metastasis[63, 64, 65]. On the contrary, MΦs with immune activating functions, including *MHCII*^{hi} MΦ, MΦ/DCs and *Ear2*^{hi} MΦ, were amplified by the two treatments, especially in caerin 1.1/1.9 group. Therefore, caerin 1.1/1.9 injection further expanded macrophages with immune activating function while reducing the immune suppressive macrophage of vaccinated and PD-1 blocked TC-1 tumour bearing mice, through mechanisms yet to be identified.

It has been found that B cells significantly promoted tumour growth in E6/E7-expressing TC-1 tumour bearing mice, while the reduction of B cells was found to stimulate more efficient anti-tumour T-cell response, suggesting immunosuppressive functions of B cells in this model[66]. B cells suppress the anti-tumour immunity through complicated interplay with tumour tissues and other lymphocytes, such as T cells, antigen-presenting cells (APCs), Tregs and myeloid-derived suppressor cells (MDSCs)[67, 68, 69]. The scRNA-seq showed that the treatment containing caerin 1.1/1.9 nearly depleted B cell population (**Supplementary File 2**), with expression of marker genes largely downregulated in general, including many genes regulating B cell differentiation and activation, such as *Ms4a1* (*Cd20*), *Fcer2a* (*Cd23*), *Cd79a* and *Ebf1*[70]. This was also reflected in proteomic analysis that antigen processing and presentation pathway was remarkably less enriched compared to that in control group, and the biological processes associated with MHCI and MHCII was insignificantly modulated by caerin 1.1/1.9 with respect to untreated or control groups (**Fig. 6**). Meanwhile, proteasome pathway was largely inhibited, due to the downregulations of *Psmb5*, *Psmb6*, *Psmb7*, *Psmd9* and *H2afz*, in TC-1 tumour treated by caerin 1.1/1.9 as suggested by proteomic analysis (**Supplementary Data 6**). A recent study found that the inhibition of proteasome caused B cells to become unable to deplete actin at the centrosome and renders them incapable of separating the centrosome from the nucleus, thus cell polarity and organisation was impaired[71]. In addition, proteomic analysis also found that proteoglycans (PGs) in cancer pathway was inhibited by caerin 1.1/1.9-containing treatment (**Supplementary Data 6**), which might also negatively affect B cell development[72].

Previously, we found that caerin 1.1/1.9 attracted NK cells to the TC-1 tumour[20]. Though the numbers were relatively low (less than 100) in the current study, NK cells were elevated significantly in caerin 1.1/1.9 group (**Supplementary File 2**). The overlapping distribution of its marker genes with $CD4^+CD8^+$ and $CD8^+$ T cells suggested certain similarity in their cellular function. We found that *Cd56*^{bright} NK cells were largely activated only in caerin 1.1/1.9 group. *Cd56*^{bright} NK cells were reported to have a regulatory role in early immune response due to the capability of producing different cytokines and shaping adaptive response [73]. Notably, scRNAseq determined *Gzmc* as the marker gene with the second highest upregulation and the largest mean expression, and there were more NK cells showing higher expression of *Gzmc* stimulated by caerin 1.1/1.9. This was consistent with the observation uncovered by the proteomic analysis that the content of *Gzmc* was increased and natural killer cell mediated cytotoxicity pathways activated significantly only in the tumour tissue of caerin 1.1/1.9 group, suggesting a higher cytotoxicity might be induced to cause more efficient cell death in TC-1 tumour, which was reflected as the enrichment of apoptosis and intrinsic pathway for apoptosis only in this group (**Supplementary Fig. 14F**). It has been found that *Gzmc* can support CTL-mediated killing via the granule exocytosis pathway during late primary alloimmune responses[74], potentially related to the mutual function shared between NK and two T cell populations. A previous study uncovered the activation of caspase-independent cell death with a mitochondrial phenotype by *Gzmc*[75], while our scRNA-seq analysis revealed the pathway, activation and myristolyation of BID and translocation to mitochondria, the second most enriched process in caerin 1.1/1.9 group.

NLR signalling activation was indicated by both scRNA-seq and proteomic analysis. *Nlrc4* acts as a downstream transcriptional target of p53 and shows potential anti-tumorigenic functions[76]. The upregulation of *Nlrp3* was shown to induce *Stat1* phosphorylation through IFNγ, thus promote an anti-tumorigenic environment[77]. The proteomic analysis identified *Stat1* only upregulated in caerin 1.1/1.9 group with significance, and it appeared as the node with the highest degree of interactions with other upregulated proteins. *Stat1* was found to act as an essential mediator of the antitumor response by inhibiting MDSC accumulation and promoting T-cell mediated immune responses in murine head and neck squamous cell carcinoma[78]. NF-kB pathway was significantly activated with the presence of caerin 1.1/1.9 (**Fig. 6G**), which might function synergistically with *Stat1* to induce more *iNOS* and *Il12*[79], thus triggering recruitment of NK cells and CTLs. This was consistent with the observation that the NK population and the activation of $CD8^+$ T cells were largely promoted, and the much higher upregulation of *Il12b* was detected in migDCs by scRNA-seq in caerin 1.1/1.9 group. These NK cells and $CD8^+$ T cells joined the C0_MΦ/DC-CCL5 to elicit apoptosis in TC-1 tumour, which was highly activated in caerin 1.1/1.9 group exclusively suggested by proteomic analysis. In addition, the co-activation of *Stat1* and *Rela* (significantly upregulated in neutrophils and migDCs) potentially triggered the expression of *iNOS*, consequently producing nitric oxide that could contribute to tumour elimination[80]. Here, insignificant upregulation (about 1.3-fold change in relative to untreated or control group) of *Nos3* in caerin 1.1/1.9 group was identified by proteomic analysis.

Taken together, therapeutic vaccination with a HPV16 E7 peptide based vaccine incorporating IL-10 receptor antibody plus PD-1 blockade induces antitumor responses, caerin 1.1/1.9 injection further expanded immune activating macrophages (*MHCII*^{hi} and *Ear*^{hi} MΦs) and NK cells, reduced immune suppressive B cells and resulted in more activated CD8+ T cells, which directly mediate proinflammatory apoptosis of tumour cells with *Stat1* playing a key role interacting with the regulators on multiple pathways. We demonstrated that caerin 1.1/1.9 containing treatment may result in improved antitumor responses. Harnessing the novel candidate genes preferentially enriched in the immune active cell populations may allow further exploration of distinct macrophages, T cells and their functions in TC-1 tumour, providing a valuable resource for researchers in the field.

Methods

Chemicals

Trifluoroacetic acid (TFA), methanol, acetonitrile (ACN), formic acid (FA), NH_4HCO_3, urea, dithiothreitol (DTT), iodoacetamide (IAA), sodium pyruvate, L-glutamine, G418, Sodium dodecyl sulfate (SDS), TRIS hydrochloride (Tris-HCl) and non-essential amino acid solution were purchased from Sigma-Alderich (St. Louis, MO). Trypsin (Mass Spec grade V5280) was purchased from Promega (Madison, WI). Ultrapure water was prepared by Milli-Q water purification system (Millipore, Bedford, MA). The TMT10plex™ Mass Tag Isobaric Labelling kit was purchased from Thermo Scientific™ (Madison, WI, USA).

Mice

Six to eight weeks old, specific pathogen free (SPF) adult female C57BL/6 (H-2b) mice were ordered from the Animal Resource Centre of Guangdong Province and kept at the Animal Facility, the first affiliated hospital of Guangdong Pharmaceutical University, Guangdong, China. Experiments were approved by and then performed in compliance with the guidelines of Animal Experimentation Ethics Committee (Ethics Approval Number: FAHGPU20160316). All mice were kept at SPF condition on a 12-hr light/12-hr dark cycle at 22°C and the humidity was 75%. 5 mice were kept each cage, provided with sterilised standard mouse food and water. TC-1 tumour bearing mice were given 1% sodium pentobarbital by *i.p.* injection when treatment was performed. Mice were sacrificed by CO_2 inhalation at the end of each experiment and confirmed by the ceasing of breath and heartbeat.

Cell line, peptide synthesis and antibodies

A murine TC-1 cell line transformed with HPV16 E6/E7 was obtained from Shanghai Institute for Cell Resources Centre, Chinese Academy of Sciences. TC-1 cells were cultured at 37°C with 5% CO_2 in complete RPMI 1640 media (GIBCO) supplemented with 10% heat inactivated fetal calf serum (FCS, GIBCO), 100 U of penicillin/mL and 100 mg of streptomycin/mL (GIBCO), 0.2 mM non-essential amino acid solution, 1.0 mM sodium pyruvate, 2 mM L-glutamine, 0.4 mg/mL G418.

Caerin 1.1 (GLLSVLGSVAKHVLPHVLPHVVPVIAEHL-NH_2) and caerin 1.9 (GLFGVLGSIAKHVLPHVVPVIAEKL-NH_2), control peptide P3 (GTELPSPPSVWFEAEFK-OH), HPV16 E7 CTL epitope RAHYNIVTF, and four overlapping peptides representing the entire HPV 16 E7 protein, EX (MHGDTPTLHEYMLDLQPETTDLYCYEQLNDSSEEE, LNDSSEEEDEIDGPAGQAEPDRAHYNIVTFCCKC, DRAHYNIVTFCCKCDSTLRLCVQSTHVDIR, CVQSTHVDIRTLEDLLMGTLGIVCPICSQKP were synthesised by Mimotopes Proprietary Limited, Wuxi, China. The purity of the peptides was >99% as determined by reverse-phase HPLC at Mimotopes. The lipopolysaccharide concentration of caerin 1.1, caerin 1.9 and P3 was 0.03, 0.03 and 0.44 EU/mL respectively, as measured by Kinetic Turbidimetric Assay by Xiamen Bioendo Technology Co., Ltd.

Rat anti-mouse anti-IL10 receptor (1B1.3), Anti-PD1 (J43) Hamster anti-mouse monoclonal antibody (MAb) and IgG Isotype control antibody LTF-2 were purchased from BioXcell, USA and stored at -80°C till further use.

Tumour challenge

TC-1 cells, at approximately 70% confluency, were harvested with 0.25% trypsin and washed repeatedly with PBS. 5×10^5 /mouse in 0.2 ml of PBS were injected subcutaneously into the left flank. Tumour sizes were assessed every 3 days using callipers to determine the average diameter of each tumour. Tumour volumes were calculated as width×width×length. Mice were sacrificed when the tumour diameter reached 20 mm.

Immunisation of mice

Three days post TC-1-challenge, six mice were immunised subcutaneously (*s.c.*) with vaccine containing either 40 µg of four overlapping HPV16E7 peptides (EX) (10 µg/each), 10 µg of monophosphoryl lipid A (MPLA) (Sigma-Aldrich), with or without 300 µg of anti-IL10R antibodies, dissolved in 100 µl of PBS, and on day 9 and 18 respectively. 300 µg of Anti-PD-1 were administered intraperitoneally(*i.p.*) on days 9 and 21 after tumour challenge (**Fig. 1**).

Tumour local administration of caerin peptide

Three days post-TC-1-challenge, when the tumours' diameters reached 3 to 5 mm, the mice either immunised or unimmunised were intratumorally injected with 30µg of caerin peptides (Caerin 1.1 and Caerin 1.9), or PBS for six consecutive days.

ELISPOT

Single spleen cell suspensions were added to membrane base 96 well ELISPOT plate (Millipore, Bedford, MA) coated with anti-IFN-*γ* (BD Harlingen, San Diego, CA). HPV16 E7 CTL epitope RAHYNIVTF was added at various concentrations and cells incubated with the peptide overnight at 37°C with 5% CO_2. The plate was incubated with detection antibody (a biotinylated anti-mouse IFN-*γ* antibody, BD Harlingen, San Diego, CA) after extensive washing in wash buffer for 2 hours at room temperature Antigen. specific IFN-*γ*

secreting cells were detected by sequential exposure of the plate to avidin–horseradish peroxidase (Sigma-Aldrich) and DAB (Sigma-Aldrich). The plate was washed, allowed to air dry overnight, foci of staining were counted by ELISPOT reader system (CTL, Germany).

Isolation of tumour infiltrating CD45+ cells

TC-1 tumour from untreated, vaccinated and PD-1 blockaded in conjunction with the injection of caerin 1.1/1.9 (molar ratio 1:1, at 39 μg/mL) or control peptide P3 mice were pooled (3 tumours/group), cut into 2×2mm pieced, digested by adding 2.35 mL of RPMI 1640, 100 μL of Enzyme D, 50 μL of Enzyme R, and 12.5 μL of Enzyme A into a gentleMACS C Tube, followed by disassociation using gentle MACS Dissociator from Miltenyi (Gladbach, Germany). After removal of dead cell and cell debris, the remaining cells were labelled with CD45 microbeads (130-110-618) and passed through LS column. The purity and viability of the CD45+ cells were more than 80% confirmed by flow cytometry and trypan blue staining.

GEM generation and barcoding

The Single Cell 3’ Protocol upgrades short read sequencers to deliver a scalable microfluidic platform for 3’ digital gene expression profiling of 500–10000 individual cells per sample. The 10x™ GemCode™ Technology samples a pool of ~750000 barcodes to separately index each cell’s transcriptome. It does so by partitioning thousands of cells into nanoliter-scale Gel Bead-In EMulsions (GEMs), where all generated cDNA shares a common 10x Barcode. Libraries are generated and sequenced from the cDNA and the 10x Barcodes are used to associate individual reads back to the individual partitions. Upon dissolution of the Single Cell 3’ Gel Bead in a GEM, primers containing (i) an Illumina® R1 sequence (read 1 sequencing primer), (ii) a 16 nt 10x Barcode, (iii) a 10 nt Unique Molecular Identifier (UMI), and (iv) a poly-dT primer sequence are released and mixed with cell lysate and Master Mix. Incubation of the GEMs then produces barcoded, full-length cDNA from poly adenylated mRNA. After incubation, the GEMs are broken and the pooled fractions are recovered.

GEM-RT clean-up and cDNA amplification

Silane magnetic beads are used to remove leftover biochemical reagents and primers from the post GEM reaction mixture. Full-length, barcoded cDNA is then amplified by PCR to generate sufficient mass for library construction.

Library construction

R1 (read 1 primer sequence) are added to the molecules during GEM incubation. P5, P7, a sample index, and R2 (read 2 primer sequence) are added during library construction via End Repair, Atailing, Adaptor Ligation, and PCR. The final libraries contain the P5 and P7 primers used in Illumina bridge amplification.

Sequencing

The Single Cell 3’ Protocol produces Illumina-ready sequencing libraries. A Single Cell 3’ Library comprises standard Illumina paired-end constructs which begin and end with P5 and P7. The Single Cell 3’ 16 bp 10x Barcode and 10 bp UMI are encoded in Read 1, while Read 2 is used to sequence the cDNA fragment. Sample index sequences are incorporated as the i7 index read. Read 1 and Read 2 are standard Illumina® sequencing primer sites used in paired-end sequencing.

Genome Alignment

Cell Ranger (http://support.10xgenomics.com/single-cell/software/overview/welcome) uses an aligner called STAR (https://github.com/alexdobin/STAR), which performs splicing-aware alignment of reads to the genome. Cell Ranger then uses the transcript annotation GTF to bucket the reads into exonic, intronic, and intergenic, and by whether the reads align (confidently) to the genome. A read is exonic if at least 50% of it intersects an exon, intronic if it is non-exonic and intersects an intron, and intergenic otherwise. Cell Ranger further aligns exonic reads to annotated transcripts, looking for compatibility. A read that is compatible with the exons of an annotated transcript, and aligned to the same strand, is considered mapped to the transcriptome. If the read is compatible with a single gene annotation, it is considered uniquely (confidently) mapped to the transcriptome. Only reads that are confidently mapped to the transcriptome are used for UMI counting.

Calling Cell Barcodes

Cell Ranger takes as input the expected number of recovered cells, *N.* Let m be a robust estimate of the maximum total UMI counts, taken as the 99th percentile of the top *N* barcodes by total UMI counts. All barcodes whose total UMI counts exceed *m*/10 are called as cells.

Depth normalisation

When combining data from multiple libraries, the read depth between libraries were equalised before merging, to reduce the batch effect introduced by sequencing. Subsample reads from higher-depth libraries until they all have an equal number of total reads per cell.

Expression QC

Seurat was used to explore QC metrics and filter cells with the following filtration.

1) 500 < gene counts < 4000 per cell.

2) UMI counts < 8000 per cell.

3) the percentage of mitochondrial genes < 10%.

Based on the number of genes identified, total UMI number and the ratio of the mitochondria gene expression in one cell, high quality cells were filtered to be included in the following subtype clustering (**Supplementary Fig. 1**). With the quality control filters, 4,648 cells (untreated tumour), 6,523 cells (caerin

1.1/1.9 treatment) and 6,409 cells (the negative control P3 treatment) were included in the analysis (**Supplementary Data 1**).

Normalising the data

After removing unwanted cells from the dataset, the next step is to normalize the data. By default, we employ a global-scaling normalization method “LogNormalise” that normalizes the gene expression measurements for each cell by the total expression, multiplies this by a scale factor (10,000 by default), and log-transforms the result. The formula is shown as follows: A gene expression level = $\log_{10}$(1 + (UMI A ÷ UMI Total) × 10000).

Clustering cells

Seurat implements a graph-based clustering approach. Distances between the cells are calculated based on previously identified PCs. Seurat approach was heavily inspired by recent manuscripts which applied graph-based clustering approaches to scRNA-seq data - SNN-Cliq[81] and CyTOF data– PhenoGraph[82]. To cluster the cells, we apply modularity optimisation techniques – SLM[83], to iteratively group cells together, with the goal of optimizing the standard modularity function.

Differentially expressed genes analysis

We used likelihood-ratio test to find differential expression for a single cluster, compared to all other cells. We identified differentially expressed genes as following criteria:

1) *P*-value ≤ 0.01.

2) Log FC ≥ 0.360674. LogFC means log fold-change of the average expression between the two groups.

3) The percentage of cells where the gene is detected in specific cluster > 25%.

Marker genes analysis

We further selected the top 20 genes as the marker genes according to the result of differentially expression genes. Then the expression distribution of each marker gene was demonstrated by using heat map and bubble diagram. The putative biological identity of each cluster was assigned by using a murine gene expression atlas[23] and the database of cell markers[24].

Constructing single cell trajectories

Single cell trajectory was analyzed using matrix of cells and gene expressions by Monocle (Version2.6.4). Monocle reduced the space down to one with two dimensions and ordered the cells (sigma = 0.001, lambda = NULL, param.gamma = 10, tol = 0.001). Once the cells were ordered, we could visualize the trajectory in the reduced dimensional space. The trajectory has a tree-like structure, including tips and branches.

Differential expression analysis in trajectories

Monocle can find genes that are differentially expressed between groups of cells and assesses the statistical signficance of those changes. We identified key genes related to the development and differentiation process with FDR<1E-5, and grouped genes with similar trends in expression, reasoning that such groups might share common biological functions and regulators.

Analysing branches in trajectories

Often, single-cell trajectories include branches. The branches occur because cells execute alternative gene expression programs. Branches appear in trajectories during development, when cells make fate choices: one developmental lineage proceeds down one path, while the other lineage produces a second path. Monocle develop BEAM to test for branch-dependent gene expression by formulating the problem as a contrast between two negative binomial GLMs.

Protein extraction, TMT-10plex labelling and high pH reversed-phase fractionation

Tumour samples was collected and directly frozen in liquid nitrogen prior to protein extraction and sample preparation. Biological triplicates were collected for each treatment. These tissues were the same biological triplicates from which the $CD45^+$ cells were extracted for scRNA-seq. The tissue samples were homogenised thoroughly in SDT buffer (4%(w/v) SDS, 100 mM Tris-HCl pH7.6, 0.1M DTT) at 4 ^oC, with the total protein contents quantified using the Pierce BCA protein assay on a NanoDrop 2000 (Thermo Fisher Scientific, Bremen, Germany). Certain amounts of samples containing 500ug of protein were subjected to trypsin digestion by the filter aided proteome preparation (FASP) described elsewhere [84]. Tryptic peptides were desalted on Sep-Pak C18 columns (Waters, Milford, MA) and lyophilised. The peptide samples (n=9) were resuspended in 30 µL of 0.5 M triethylammonium bicarbonate (pH 8.5) and quantified on the NanoDrop 2000 using OD280 nm. Then, the samples containing 100 µg peptides were transferred to Eppendorf tubes and labelled by TMT10-plex following the manufacturer's instruction. Briefly, the TMT labelling reagents were dissolved in 41 µL acetonitrile per vial and added to the samples. The reaction was incubated for 1 h at RT and quenched by 5% hydroxylamine. In this study, 126, 127N and 127C were used to label untreated tumour samples; 128N, 128C and 129N were used to label the treatments with caerin peptides; the treatments with the addition of P3 were labelled using 129C, 130N and130C, respectively. The labelled samples were mixed and fractionated using a Pierce^{TM} high pH Reversed-Phase Peptide Fractionation Kit (Thermo Fisher Scientific, U.S.) according to manufacturer's instruction. In brief, the columns were first conditioned using 0.1%TFA/100%ACN and loaded with samples, which were then washed using MilliQ water by centrifugation at 3,000g. Finally, the fractions were eluted by increasing concentrations of ACN in ACN/ Triethylamine (0.1%) from 5% to 50%. All fractions were lyophilised on a SpeedVac and resuspended 12 µL 0.1%FA for LC-MS/MS analysis.

Easy nLC tandem Q-Exactive MS/MS analyses

A 10 µl of sample solution was loaded onto a two dimensional EASY-nLC1000 system coupled to a Q Exactive Hybrid Quadrupole-Orbitrap Mass Spectrometer (Thermo Scientific). In the nanoLC separation system, mobile phase A solution containing 0.1 % formic acid in water, and mobile phase B solution containing 84 % acetonitrile and 0.1 % formic acid. Before peptide loading, the columns were pre-equilibrated with 95 % mobile phase A for 30 min. The samples were first injected into the sample loading column (Thermo Scientific Acclaim PepMap100, 100µm × 2cm, nanoViper C18), then fractionated by the analytic column (Thermo scientific EASY column, 10cm, ID75µm, 3µm, C18-A2) Thermo EASY SC200 trap column (RP-C18, 3 µm, 100 mm × 75 µm). The phosphopeptides were first transferred to the Thermo scientific EASY column (2cm × 100 µm 5 µm-C18) and then separated via the trap column using a gradient of 0–55 % mobile phase B for 220 min. Then, the columns were rinsed with 100 % mobile phase B for 8 min and re-equilibrated to the initial conditions for 12 min. The flow rate of the above procedures was 300 nl/min. The samples were then analysed on a Q-Exactive Obitrap mass spectrometer (Thermo

Fisher Scientific, Waltham, MA, USA). The ion spray voltage was set to 5500 V, the declustering potential was set to 100 V, the curtain gas flow was set at 30, ion source gas 1 was set at 40, the ion source gas 2 was set at 50 and spray temperature was set at 450°C. The mass spectrometer acquired the mass spectral data in an Information Dependant Acquisition, IDA mode. Full scan MS data was acquired over the mass range 300-1800 with a resolution of 70,000 at 200 m/z. AGC (Automatic gain control) target was set at 10^6, the maximum IT was set at 50ms and the dynamic exclusion was set at 60.0s. In every full scan, twenty MS/MS spectra were obtained. The MS/MS activation type was HCD and the isolation window was2 m/z. The resolution of MS/MS was 35,000 at 200 m/z, the normalized Collision Energy was set at 30 and the underfill was set at 0.1%.

Protein identification and quantification

The MS/MS data was searched against Swissprot Mouse (76,413 sequences, downloaded on Dec 12, 2014) database for protein identification using Mascot2.2 (Matrix Science, London, UK) and Proteome Discoverer1.4 software (Thermo Fisher Scientific, Waltham, MA, USA) with the following search settings: enzyme trypsin; two missed cleavage sites; precursor mass tolerance 20 ppm; fragment mass tolerance 0.1 Da; fixed modifications: Carbamidomethyl (C), TMT 10plex (N-term),TMT10 plex (K); variable modifications: oxidation (M) , TMT 10plex (Y). The results of the search were further submitted to generate the final report using a cut-off of 1% FDR on peptide levels and only unique peptides were used for protein quantitation. All peptide ratios were normalised by the median protein ratio, and the median protein ratio was 1 after the normalisation. The protein showing a fold change≥1.2 (upregulation≥ 1.2 or downregulation ≤0.83) compared to the untreated group and the *P*-value<0.05 were considered significantly regulated by the treatment and included in further analysis.

Protein-protein interaction (PPI) analysis

Interactions among significantly regulated proteins were predicted using STRING[85]. STRING provides a critical assessment and integration of protein-protein interactions from multiple resources, including

direct (physical) as well as indirect (functional) associations. A spring model to generate the network images. All resources were selected to generate the network and 'confidence' was used as the meaning of network edges and the required interaction score of 0.700 was selected for all PPI, to highlight the most confident interactions. Neither the 1st nor 2nd shell of the PPI was included in this study. Protein without any interaction with other proteins was excluded from displaying in the network.

Biological process and pathway analysis

The enrichment of biological processes, WikiPathways[86], KEGG pathways[87] and Reactome pathways[88] in the significantly upregulated genes (*P*-value<0.05) of different cell populations/subpopulations determined by scRNAseq, or proteins significantly upregulated (fold change >1.2 and *P*-value<0.05) by the treatments with respective to untreated group derived from quantitative proteomics, were analysed by Enrichr (http://amp.pharm.mssm.edu/Enrichr/). In addition, the proteins determined to be differentially expressed were analysed by the online tool Innate DB (https://www.innatedb.ca/index.jsp), to further investigate the modulation of immune response relevant pathways. In the analysis, the up-/down-regulation of key regulators identified in different treatments, with a fold change ≥2 and P-value<0.05, were used to predict the activation/inhibition of signalling pathways.

Declarations

Acknowledgement

This study was supported by Deng Feng project of Foshan First People's Hospital (2019A008), Foshan municipal Government (2015AG1003), Guangdong Provincial Government (2016A020213001) of China, National Science Foundation of China (31971355) and Australian Research Council Discovery Project (ARC DP180103694). The funders were not involved in the design, data collection and analysis, preparation or publication of the manuscript. We thank Professor Abigail Elizur for her valuable advice and support. We are grateful for the sequencing platform and/or bioinformation analysis and proteomic experiment of Gene Denovo Biotechnology Co., Ltd (Guangzhou, China) and Applied Protein Technology, Co Ltd (Shanghai, China).

Contributions

Conceptualisation and design: T.W. and X.L.; Experimental work: G.N., Y.L., S.C. and X.W.; Data process, curation and visualisation: H.L., T.W. and X.L.; Analysis and interpretation: T.W., X.L. and I.F.; Writing-original draft preparation: T.W. and X.L.; Writing-review and editing: C.F., T.W., X.L., and I.F.; project administration: X.W. All authors reviewed the paper.

Ethics declarations

The authors declare no competing interests.

Data availability

The scRNA-seq data is available on the Institute Single Cell Portal [https://singlecell.broadinstitute.org/single_cell] under accession number SCP1093. The mass spectrometry proteomics data have been deposited to the ProteomeXchange Consortium via the PRIDE[89] partner repository with the dataset identifier PXD021264.

References

1. Zhou C, Tuong ZK, Frazer IH. Papillomavirus Immune Evasion Strategies Target the Infected Cell and the Local Immune System. *Front Oncol* **9**, 682 (2019).

2. Tuyaerts S*, et al.* PRIMMO study protocol: a phase II study combining PD-1 blockade, radiation and immunomodulation to tackle cervical and uterine cancer. *BMC Cancer* **19**, 506 (2019).

3. Ni G*, et al.* Human papillomavirus infection among head and neck squamous cell carcinomas in southern China. *PloS one* **14**, e0221045 (2019).

4. Ribas A, Wolchok JD. Cancer immunotherapy using checkpoint blockade. *Science* **359**, 1350-1355 (2018).

5. Saglam O, Conejo-Garcia J. PD-1/PD-L1 immune checkpoint inhibitors in advanced cervical cancer. *Integr Cancer Sci Ther* **5**, (2018).

6. Borcoman E, Le Tourneau C. Pembrolizumab in cervical cancer: latest evidence and clinical usefulness. *Ther Adv Med Oncol* **9**, 431-439 (2017).

7. Tondini E*, et al.* A poly-neoantigen DNA vaccine synergizes with PD-1 blockade to induce T cell-mediated tumor control. *Oncoimmunology* **8**, 1652539 (2019).

8. Chandra J*, et al.* DNA Vaccine Encoding HPV16 Oncogenes E6 and E7 Induces Potent Cell-mediated and Humoral Immunity Which Protects in Tumor Challenge and Drives E7-expressing Skin Graft Rejection. *J Immunother* **40**, 62-70 (2017).

9. Curran MA, Glisson BS. New Hope for Therapeutic Cancer Vaccines in the Era of Immune Checkpoint Modulation. *Annu Rev Med* **70**, 409-424 (2019).

10. Ott PA*, et al.* An immunogenic personal neoantigen vaccine for patients with melanoma. *Nature* **547**, 217-221 (2017).

11. Kenter GG*, et al.* Vaccination against HPV-16 oncoproteins for vulvar intraepithelial neoplasia. *N Engl J Med* **361**, 1838-1847 (2009).

12. van Poelgeest MI*, et al.* HPV16 synthetic long peptide (HPV16-SLP) vaccination therapy of patients with advanced or recurrent HPV16-induced gynecological carcinoma, a phase II trial. *Journal of translational medicine* **11**, 88 (2013).

13. Pan X*, et al.* Synthesized natural peptides from amphibian skin secretions increase the efficacy of a therapeutic vaccine by recruiting more T cells to the tumour site. *BMC complementary and alternative medicine* **19**, 163 (2019).

14. Llopiz D*, et al.* Vaccine-induced but not tumor-derived Interleukin-10 dictates the efficacy of Interleukin-10 blockade in therapeutic vaccination. *Oncoimmunology* **5**, e1075113 (2016).

15. Gasser S, Lim LHK, Cheung FSG. The role of the tumour microenvironment in immunotherapy. *Endocr Relat Cancer* **24**, T283-T295 (2017).

16. Engblom C, Pfirschke C, Pittet MJ. The role of myeloid cells in cancer therapies. *Nature reviews Cancer* **16**, 447-462 (2016).

17. Mantovani A, Marchesi F, Malesci A, Laghi L, Allavena P. Tumour-associated macrophages as treatment targets in oncology. *Nature reviews Clinical oncology* **14**, 399-416 (2017).

18. Gordon SR*, et al.* PD-1 expression by tumour-associated macrophages inhibits phagocytosis and tumour immunity. *Nature* **545**, 495-499 (2017).

19. Ni G*, et al.* Comparative Proteomic Study of the Antiproliferative Activity of Frog Host-Defence Peptide Caerin 1.9 and Its Additive Effect with Caerin 1.1 on TC-1 Cells Transformed with HPV16 E6 and E7. *Biomed Res Int* **2018**, 7382351 (2018).

20. Ma B*, et al.* Topical application of temperature-sensitive caerin 1.1 and 1.9 gel inhibits TC-1 tumor growth in mice. *American journal of translational research* **12**, 191-202 (2020).

21. Ni G*, et al.* Host-Defense Peptides Caerin 1.1 and 1.9 Stimulate TNF-Alpha-Dependent Apoptotic Signals in Human Cervical Cancer HeLa Cells. **8**, (2020).

22. VanCompernolle SE*, et al.* Antimicrobial peptides from amphibian skin potently inhibit human immunodeficiency virus infection and transfer of virus from dendritic cells to T cells. *Journal of virology* **79**, 11598-11606 (2005).

23. Hume DA, Summers KM, Raza S, Baillie JK, Freeman TC. Functional clustering and lineage markers: insights into cellular differentiation and gene function from large-scale microarray studies of purified primary cell populations. *Genomics* **95**, 328-338 (2010).

24. Zhang X*, et al.* CellMarker: a manually curated resource of cell markers in human and mouse. *Nucleic acids research* **47**, D721-d728 (2019).

25. Guilliams M*, et al.* Unsupervised High-Dimensional Analysis Aligns Dendritic Cells across Tissues and Species. *Immunity* **45**, 669-684 (2016).

26. Van Hove H*, et al.* A single-cell atlas of mouse brain macrophages reveals unique transcriptional identities shaped by ontogeny and tissue environment. *Nature neuroscience* **22**, 1021-1035 (2019).

27. Schwalie PC*, et al.* A stromal cell population that inhibits adipogenesis in mammalian fat depots. *Nature* **559**, 103-108 (2018).

28. Han JH*, et al.* IFITM6 expression is increased in macrophages of tumor-bearing mice. *Oncology reports* **25**, 531-536 (2011).

29. Lin JD*, et al.* Single-cell analysis of fate-mapped macrophages reveals heterogeneity, including stem-like properties, during atherosclerosis progression and regression. *JCI insight* **4**, (2019).

30. Cassetta L*, et al.* Human Tumor-Associated Macrophage and Monocyte Transcriptional Landscapes Reveal Cancer-Specific Reprogramming, Biomarkers, and Therapeutic Targets. *Cancer cell* **35**, 588-602.e510 (2019).

31. Qi L*, et al.* IL-10 secreted by M2 macrophage promoted tumorigenesis through interaction with JAK2 in glioma. *Oncotarget* **7**, 71673-71685 (2016).

32. Kudo Y*, et al.* Matrix metalloproteinase-13 (MMP-13) directly and indirectly promotes tumor angiogenesis. *The Journal of biological chemistry* **287**, 38716-38728 (2012).

33. He MK*, et al.* Matrix metalloproteinase 12 expression is associated with tumor FOXP3(+) regulatory T cell infiltration and poor prognosis in hepatocellular carcinoma. *Oncology letters* **16**, 475-482 (2018).

34. de Boniface J, Mao Y, Schmidt-Mende J, Kiessling R, Poschke I. Expression patterns of the immunomodulatory enzyme arginase 1 in blood, lymph nodes and tumor tissue of early-stage breast cancer patients. *Oncoimmunology* **1**, 1305-1312 (2012).

35. Grzywa TM*, et al.* Myeloid Cell-Derived Arginase in Cancer Immune Response. *Frontiers in immunology* **11**, 938 (2020).

36. Villani AC*, et al.* Single-cell RNA-seq reveals new types of human blood dendritic cells, monocytes, and progenitors. *Science (New York, NY)* **356**, (2017).

37. Álvarez B*, et al.* Characterization of the Porcine CLEC12A and Analysis of Its Expression on Blood Dendritic Cell Subsets. *Frontiers in immunology* **11**, 863 (2020).

38. Torossian F*, et al.* Macrophage-derived oncostatin M contributes to human and mouse neurogenic heterotopic ossifications. *JCI insight* **2**, (2017).

39. De Plaen IG, Han XB, Liu X, Hsueh W, Ghosh S, May MJ. Lipopolysaccharide induces CXCL2/macrophage inflammatory protein-2 gene expression in enterocytes via NF-kappaB activation: independence from endogenous TNF-alpha and platelet-activating factor. *Immunology* **118**, 153-163 (2006).

40. Roy S*, et al.* Redefining the transcriptional regulatory dynamics of classically and alternatively activated macrophages by deepCAGE transcriptomics. *Nucleic acids research* **43**, 6969-6982 (2015).

41. Huang C*, et al.* Proteomic Identification of Interferon-Induced Proteins with Tetratricopeptide Repeats as Markers of M1 Macrophage Polarization. *Journal of proteome research* **17**, 1485-1499 (2018).

42. Poczobutt JM*, et al.* Expression Profiling of Macrophages Reveals Multiple Populations with Distinct Biological Roles in an Immunocompetent Orthotopic Model of Lung Cancer. *Journal of immunology (Baltimore, Md : 1950)* **196**, 2847-2859 (2016).

43. Cochain C*, et al.* Single-Cell RNA-Seq Reveals the Transcriptional Landscape and Heterogeneity of Aortic Macrophages in Murine Atherosclerosis. *Circulation research* **122**, 1661-1674 (2018).

44. Hrdinka M, Yabal M. Inhibitor of apoptosis proteins in human health and disease. *Genes and immunity* **20**, 641-650 (2019).

45. Nalepa G*, et al.* The tumor suppressor CDKN3 controls mitosis. *The Journal of cell biology* **201**, 997-1012 (2013).

46. Grinenko T*, et al.* Hematopoietic stem cells can differentiate into restricted myeloid progenitors before cell division in mice. *Nature communications* **9**, 1898 (2018).

47. Geng A*, et al.* KIF20A/MKLP2 regulates the division modes of neural progenitor cells during cortical development. *Nature communications* **9**, 2707 (2018).

48. Kool M*, et al.* Facilitated antigen uptake and timed exposure to TLR ligands dictate the antigen-presenting potential of plasmacytoid DCs. *Journal of leukocyte biology* **90**, 1177-1190 (2011).

49. Zhang J*, et al.* Characterization of Siglec-H as a novel endocytic receptor expressed on murine plasmacytoid dendritic cell precursors. *Blood* **107**, 3600-3608 (2006).

50. Marçais A, Coupet CA, Walzer T, Tomkowiak M, Ghittoni R, Marvel J. Cell-autonomous CCL5 transcription by memory CD8 T cells is regulated by IL-4. *Journal of immunology (Baltimore, Md : 1950)* **177**, 4451-4457 (2006).

51. Pizzolato G*, et al.* Single-cell RNA sequencing unveils the shared and the distinct cytotoxic hallmarks of human TCRVδ1 and TCRVδ2 γδ T lymphocytes. *Proceedings of the National Academy of Sciences of the United States of America* **116**, 11906-11915 (2019).

52. Wein AN*, et al.* CXCR6 regulates localization of tissue-resident memory CD8 T cells to the airways. *The Journal of experimental medicine* **216**, 2748-2762 (2019).

53. Weng NP, Araki Y, Subedi K. The molecular basis of the memory T cell response: differential gene expression and its epigenetic regulation. *Nature reviews Immunology* **12**, 306-315 (2012).

54. Araki K*, et al.* Translation is actively regulated during the differentiation of CD8(+) effector T cells. *Nature immunology* **18**, 1046-1057 (2017).

55. Cannons JL*, et al.* 4-1BB ligand induces cell division, sustains survival, and enhances effector function of CD4 and CD8 T cells with similar efficacy. *Journal of immunology (Baltimore, Md : 1950)* **167**, 1313-1324 (2001).

56. Verdeil G, Puthier D, Nguyen C, Schmitt-Verhulst AM, Auphan-Anezin N. STAT5-mediated signals sustain a TCR-initiated gene expression program toward differentiation of CD8 T cell effectors. *Journal of immunology (Baltimore, Md : 1950)* **176**, 4834-4842 (2006).

57. Cao X*, et al.* Interleukin 12 stimulates IFN-gamma-mediated inhibition of tumor-induced regulatory T-cell proliferation and enhances tumor clearance. *Cancer research* **69**, 8700-8709 (2009).

58. Liu NQ*, et al.* Ferritin heavy chain in triple negative breast cancer: a favorable prognostic marker that relates to a cluster of differentiation 8 positive (CD8+) effector T-cell response. *Molecular & cellular proteomics : MCP* **13**, 1814-1827 (2014).

59. Wakim LM, Gupta N, Mintern JD, Villadangos JA. Enhanced survival of lung tissue-resident memory CD8⍰ T cells during infection with influenza virus due to selective expression of IFITM3. *Nature immunology* **14**, 238-245 (2013).

60. Gentles AJ*, et al.* The prognostic landscape of genes and infiltrating immune cells across human cancers. *Nature medicine* **21**, 938-945 (2015).

61. Arlauckas SP*, et al.* Arg1 expression defines immunosuppressive subsets of tumor-associated macrophages. *Theranostics* **8**, 5842-5854 (2018).

62. Mantovani A, Allavena P. The interaction of anticancer therapies with tumor-associated macrophages. *The Journal of experimental medicine* **212**, 435-445 (2015).

63. Kessenbrock K, Plaks V, Werb Z. Matrix metalloproteinases: regulators of the tumor microenvironment. *Cell* **141**, 52-67 (2010).

64. Pucci F*, et al.* PF4 Promotes Platelet Production and Lung Cancer Growth. *Cell reports* **17**, 1764-1772 (2016).

65. Chen LH, Liao CY, Lai LC, Tsai MH, Chuang EY. Semaphorin 6A Attenuates the Migration Capability of Lung Cancer Cells via the NRF2/HMOX1 Axis. *Scientific reports* **9**, 13302 (2019).

66. Tang A*, et al.* B cells promote tumor progression in a mouse model of HPV-mediated cervical cancer. *International journal of cancer* **139**, 1358-1371 (2016).

67. Tedder TF. B10 cells: a functionally defined regulatory B cell subset. *Journal of immunology (Baltimore, Md : 1950)* **194**, 1395-1401 (2015).

68. Bodogai M*, et al.* Immunosuppressive and Prometastatic Functions of Myeloid-Derived Suppressive Cells Rely upon Education from Tumor-Associated B Cells. *Cancer research* **75**, 3456-3465 (2015).

69. Rosser EC, Mauri C. Regulatory B cells: origin, phenotype, and function. *Immunity* **42**, 607-612 (2015).

70. Park J*, et al.* Single-cell transcriptomics of the mouse kidney reveals potential cellular targets of kidney disease. *Science (New York, NY)* **360**, 758-763 (2018).

71. Ibañez-Vega J, Del Valle Batalla F, Saez JJ, Soza A, Yuseff MI. Proteasome Dependent Actin Remodeling Facilitates Antigen Extraction at the Immune Synapse of B Cells. *Frontiers in immunology* **10**, 225 (2019).

72. Reijmers RM, Spaargaren M, Pals ST. Heparan sulfate proteoglycans in the control of B cell development and the pathogenesis of multiple myeloma. *The FEBS journal* **280**, 2180-2193 (2013).

73. Poli A, Michel T, Thérésine M, Andrès E, Hentges F, Zimmer J. CD56bright natural killer (NK) cells: an important NK cell subset. *Immunology* **126**, 458-465 (2009).

74. Getachew Y, Stout-Delgado H, Miller BC, Thiele DL. Granzyme C supports efficient CTL-mediated killing late in primary alloimmune responses. *Journal of immunology (Baltimore, Md : 1950)* **181**, 7810-7817 (2008).

75. Chowdhury D, Lieberman J. Death by a thousand cuts: granzyme pathways of programmed cell death. *Annual review of immunology* **26**, 389-420 (2008).

76. Sadasivam S, Gupta S, Radha V, Batta K, Kundu TK, Swarup G. Caspase-1 activator Ipaf is a p53-inducible gene involved in apoptosis. *Oncogene* **24**, 627-636 (2005).

77. Zaki MH, Vogel P, Body-Malapel M, Lamkanfi M, Kanneganti TD. IL-18 production downstream of the Nlrp3 inflammasome confers protection against colorectal tumor formation. *Journal of immunology (Baltimore, Md : 1950)* **185**, 4912-4920 (2010).

78. Ryan N*, et al.* STAT1 inhibits T-cell exhaustion and myeloid derived suppressor cell accumulation to promote antitumor immune responses in head and neck squamous cell carcinoma. *Int J Cancer* **146**, 1717-1729 (2020).

79. Dai R, Phillips RA, Karpuzoglu E, Khan D, Ahmed SA. Estrogen regulates transcription factors STAT-1 and NF-kappaB to promote inducible nitric oxide synthase and inflammatory responses. *Journal of immunology (Baltimore, Md : 1950)* **183**, 6998-7005 (2009).

80. Farlik M*, et al.* Nonconventional initiation complex assembly by STAT and NF-kappaB transcription factors regulates nitric oxide synthase expression. *Immunity* **33**, 25-34 (2010).

81. Xu C, Su Z. Identification of cell types from single-cell transcriptomes using a novel clustering method. *Bioinformatics (Oxford, England)* **31**, 1974-1980 (2015).

82. Levine JH*, et al.* Data-Driven Phenotypic Dissection of AML Reveals Progenitor-like Cells that Correlate with Prognosis. *Cell* **162**, 184-197 (2015).

83. Blondel VD, Guillaume J-L, Lambiotte R, Lefebvre E. Fast unfolding of communities in large networks. *J Stat Mech* **2008**, P10008 (2008).

84. Wisniewski JR, Zougman A, Nagaraj N, Mann M. Universal sample preparation method for proteome analysis. *Nat Methods* **6**, 359-362 (2009).

85. Szklarczyk D*, et al.* STRING v10: protein-protein interaction networks, integrated over the tree of life. *Nucleic acids research* **43**, D447-452 (2015).

86. Kutmon M*, et al.* WikiPathways: capturing the full diversity of pathway knowledge. *Nucleic acids research* **44**, D488-494 (2016).

87. Kanehisa M, Goto S. KEGG: kyoto encyclopedia of genes and genomes. *Nucleic acids research* **28**, 27-30 (2000).

88. Croft D*, et al.* The Reactome pathway knowledgebase. *Nucleic acids research* **42**, D472-477 (2014).

89. Perez-Riverol Y*, et al.* The PRIDE database and related tools and resources in 2019: improving support for quantification data. *Nucleic acids research* **47**, D442-d450 (2019).

Figures

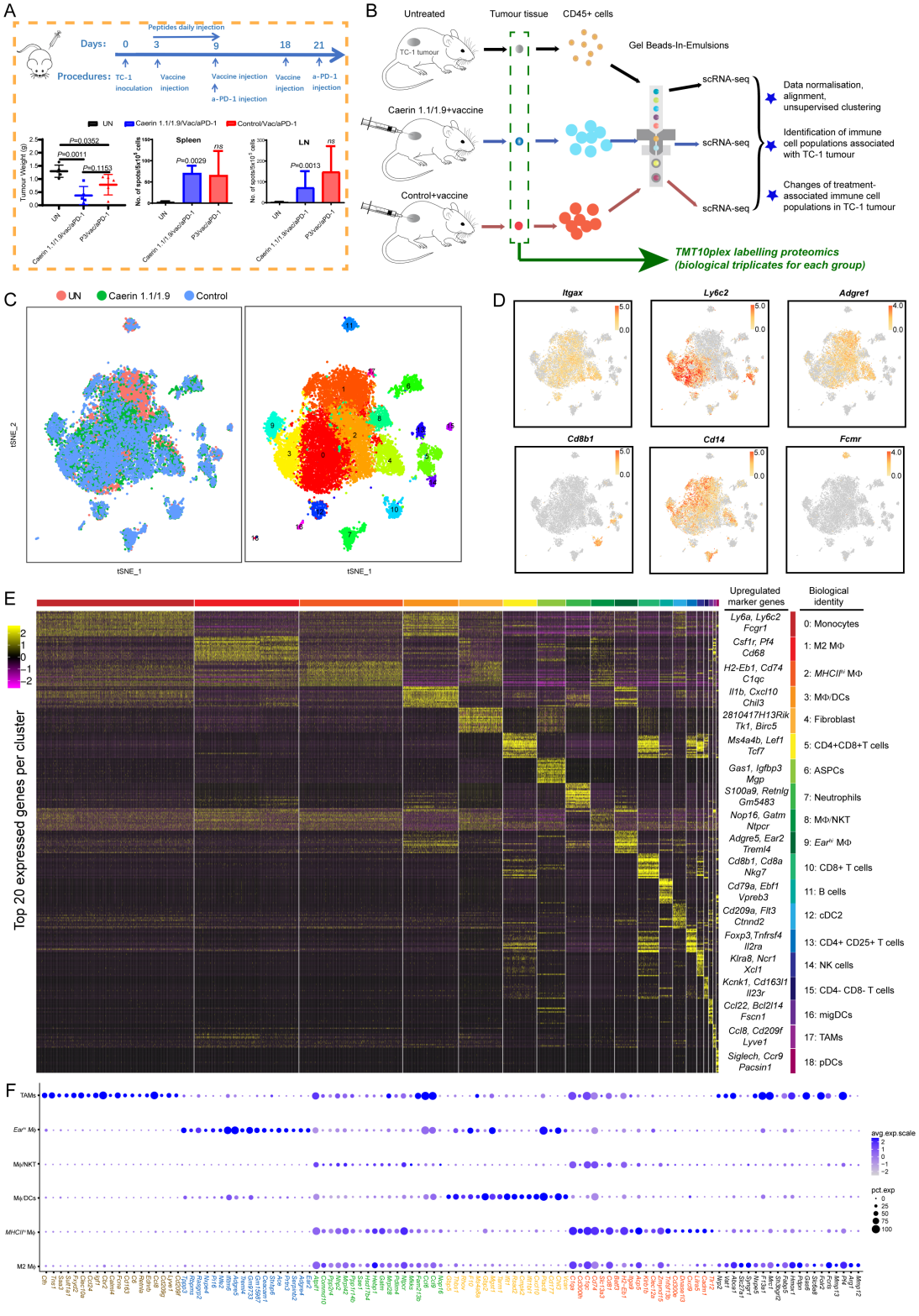

Figure 1

Identification of immune cell populations of TC-1 tumour by single-cell RNA sequencing. (A) Timeline of immunisation of TC-1 bearing mice. 30 days post tumour challenge, spleens and draining lymph nodes from control and immunised, and PD-1 blocked TC-1 tumour bearing mice, treated with caerin 1.1 and caerin 1.9 or control peptide (P3)were isolated, single cells made and subsequently cultured in the presence of HPV16 E7 CTL epitope RAHYNIVTF overnight. ELIspot assay was performed as described in

the material and methods. Left: Tumour weight; Middle: Splenic HPV16E7 specific CD8+ T cells; Right: Draining lymph node HPV16E7 specific CD8+ T cells. (B) Schematic diagram of the experimental design (including injection procedure) and data processing. (C) t-Stochastic neighbour embedding (t-SNE) representation of aligned gene expression data in single cells extracted from untreated (n=4,011), vaccination plus caerin 1.1/1.9 (n=5,685) or P3 (n=5,415) of TC-1 bearing mice showing cellular origin (top) and partition into 19 distinct clusters (bottom). (D) Gene expression patterns projected onto t-SNE plots of Itgax, Ly6C2, Adgre1, Cd8b1, Cd14, and Fcmr (scale: log-transformed gene expression). (E) Heatmap showing the 20 most upregulated genes (ordered by decreasing p value) in each cluster defined in (C) and selected enriched genes used for biological identification of each cluster (scale: log2 fold change). MΦ represents macrophage; ASPC, adipogenic stem and precursor cell; NKT, natural killer T cells; cDC, conventional dendritic cell; NK, natural killer cell; migDC, migratory dendritic cell; TAM, tumour-associated macrophage; and pDC, plasmacytoid dendritic cell. (F) Bubble map of marker gene expression distribution in different macrophage populations, including M2 MΦ, MHCIIhi MΦ, MΦ/DCs, MΦ/NKT, Earhi MΦ and TAM. The bubble size represents the ratio of the sum of the expression levels of the marker genes in a certain subpopulation to the sum of their expression levels in all cells, while the bubble colour represents the average expression of the marker genes in the cell population.

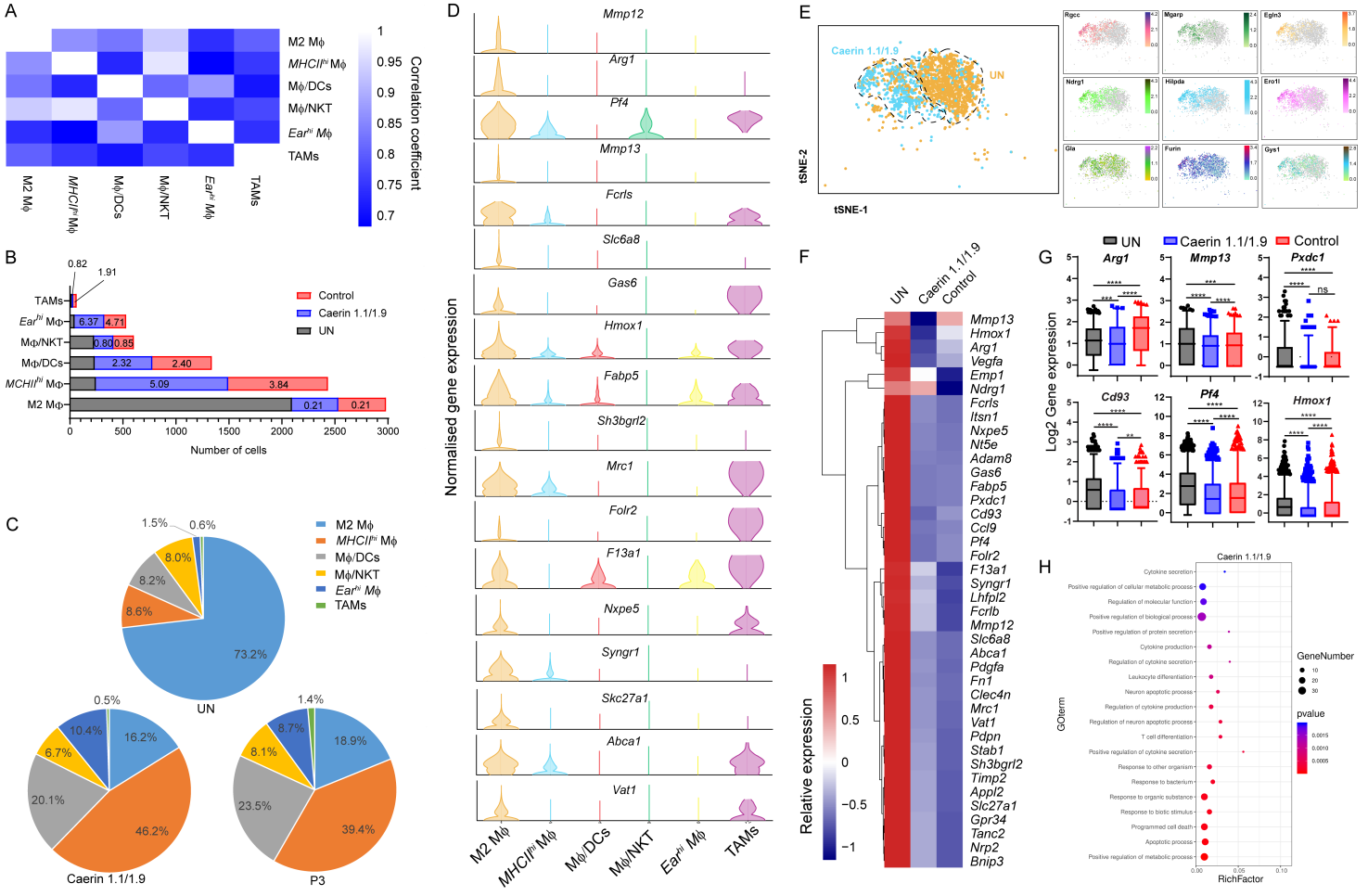

Figure 2

Immunisation increased immuno-active macrophage populations. (A) Correlation analysis among six macrophage populations. (B) The comparison of the number of cells assigned to each macrophage in different groups (untreated, caerin 1.1/1.9 and P3), and the fold change in cell numbers of two treatments in relative to untreated group was displayed on the bars. (C) The proportions of different macrophages in each group. (D) The comparison of the normalised expression of selected M2 MΦ marker genes and other macrophages. (E) t-SNE representation of aligned gene expression data of M2 MΦ and selected genes (including Rgcc, Mgarp, Egln3, Ndrg1, Hilpda, Ero1l, Gla, Furin and Gys1) from untreated and caerin 1.1/1.9 groups. (F) Relative expression comparison of the top 40 marker genes of M2 MΦ amongst three groups. (G) Statistical analysis of the expression (Log2 value) of Arg1, Mmp13, Pxdc1, Cd93, Pf4 and Hmox1. (H) Biological processes enriched in M2 MΦ population post the treatment containing caerin 1.1/1.9.

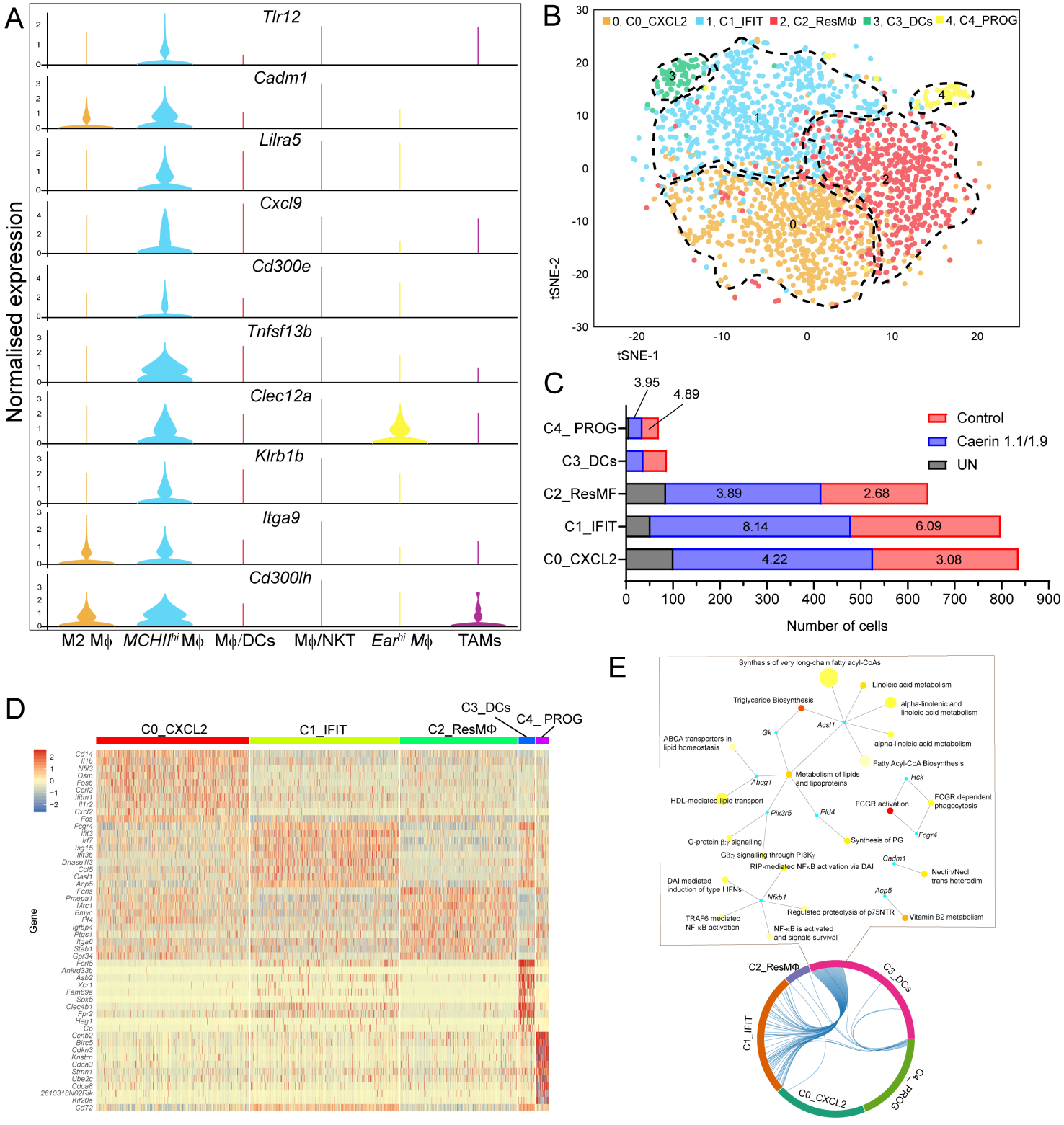

Figure 3

Immunisation in combination with PD-1 and IL10 blockade, and the injection of caerin 1.1/1.9 or P3 changed the heterogeneity of MHCIIhi MΦ population. (A) Comparison of normalised expression of selected marker genes of MHCIIhi MΦ in all MΦ populations. (B) 2D t-SNE distributions of five subpopulations of MHCIIhi MΦ. (C) Comparison of the cell numbers of subpopulations in untreated, caerin 1.1/1.9 or P3 groups. The fold changes of cell number in treatment groups with respect to

untreated group were displayed on the bars. (D) Heatmap showing the 10 most upregulated genes (ordered by decreasing p value) in each cluster defined in (B) and selected enriched genes used for biological identification of each cluster (scale: Log2 fold change). (E) Biological process network based on genes that are commonly upregulated between subpopulations C1_MHCIIhi-IFIT and C3_MHCIIhi-DCs.

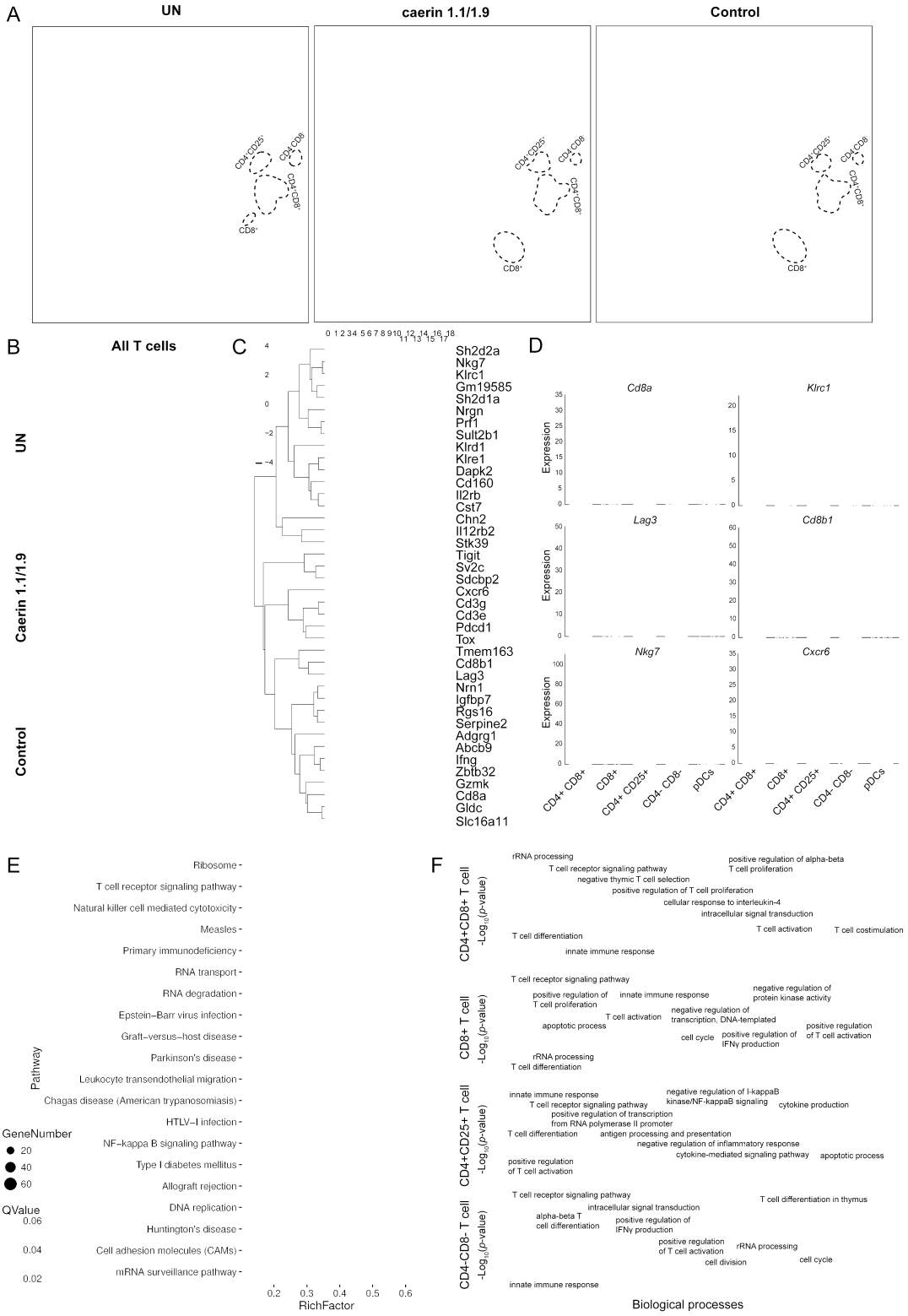

Figure 4

Comparison of TC-1 tumour infiltrating T cell populations with the caerin 1.1/1.9 or P3 peptide treatments. (A) 2D visualisation of cell populations inferred from RNA-seq data for all CD45+ cells in untreated and treated with caerin 1.1/1.9 or P3; cell types with significant changes due to the treatments were featured. Colour coded as indicated. (B) Proportions of CD4+CD8+, CD8+, CD4+CD25+ and CD4-CD8- cells within T cells extracted from the TC-1 tumour. (C) Hierarchy clustering of the top 40 marker genes of CD8+ T cells in comparison with other types of T cells. (D) Violin plots compare the gene expression of selected genes showing statistically significant upregulation in CD8+ T cells to other T cell populations and pDCs, including Cd8a, Klrc1, Lag3, Cd8b1, Nkg7 and Cxcr6. (E) The top 20 KEGG pathways enriched in CD8+ T cells. (F) Gene ontology enrichment analysis of biological processes in T cells in the TC-1 tumour. Top 25 enriched biological processes in four T cell subsets were compared in terms of P-value and gene numbers, respectively.

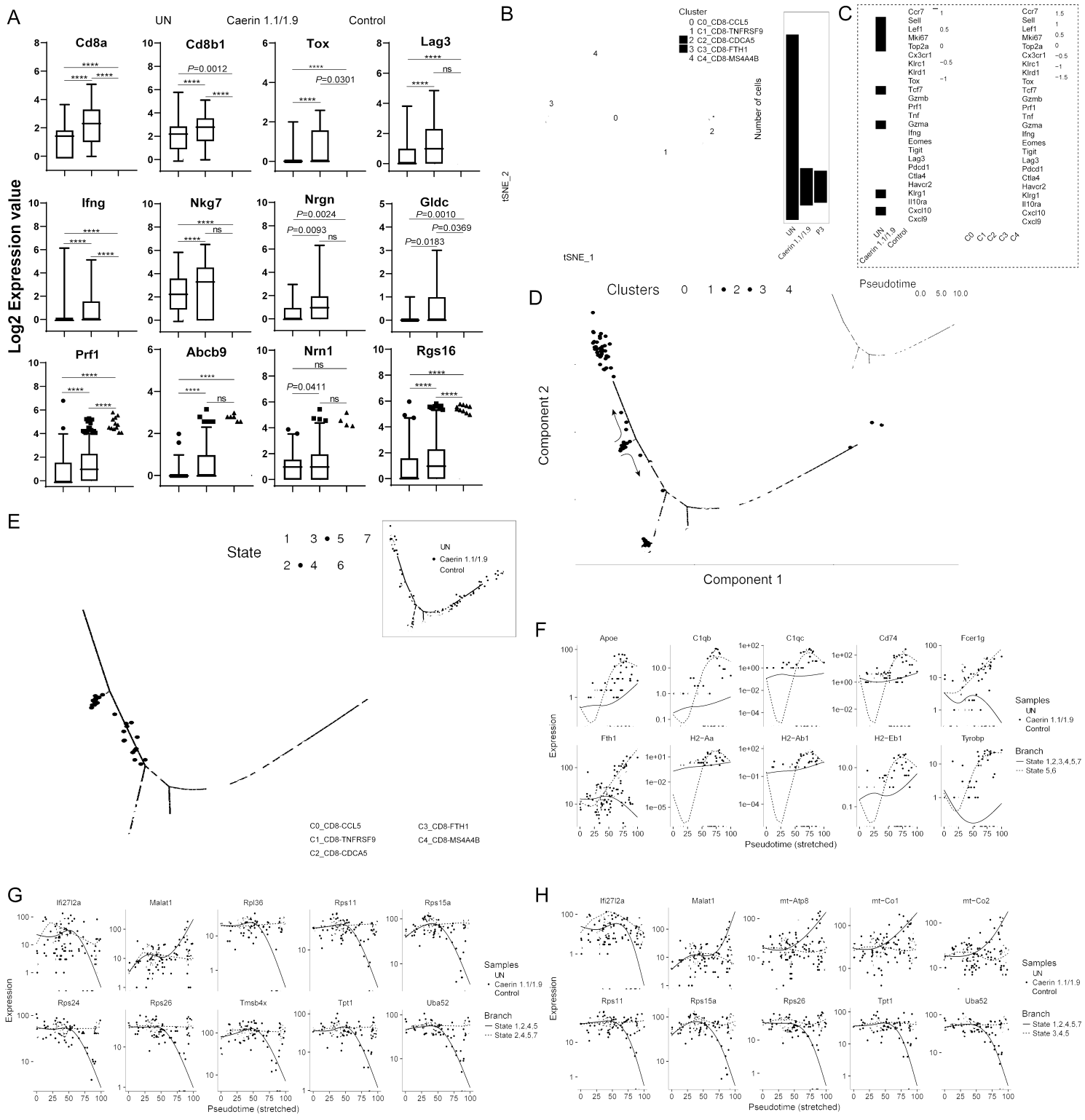

Figure 5

Comparison of CD8+ T cell marker genes with two treatments and state transition analysis based on integrated expression in subpopulations. (A) The expressions (log2 value) of Cd8a, Cd8b1, Tox, Lag3, Ifng, Nkg7, Nrgn, Gldc, Prf1, Abcb9, Nrn1 and Rgs16 in untreated tumours, treatments containing caerin 1.1/1.9 or P3. (B) The analysis of subpopulations of CD8+ T cell and the number of cells under the aforementioned three conditions. (C) The heatmaps compared the average expressions of selected genes

in untreated and treated tumour, and in five subpopulations. (D) The ordering of CD8+ T cell subpopulations along pseudotime in a two-dimensional state-space defined by Monocle3. Cell orders are inferred from the expression of most dispersed genes across CD8+ T cell subpopulations. Each point corresponds to a single cell, and each colour represents a T cell subpopulation. Cells on the same or neighbouring branches are expected to be more hierarchically related. (E) Developmental states of CD8+ T cells inferred by pseudotime. The space distribution of cells is defined in (B). Each colour represents a distinct state on the trajectory generated by Monocle. Pie charts show the proportion of cell clusters at the state when multiple clusters involved. The top 10 genes differentially expressed in different states on branch 1 (F), 2 (G) and 3 (H) along with stretched pseudotime with respect to different treatments.

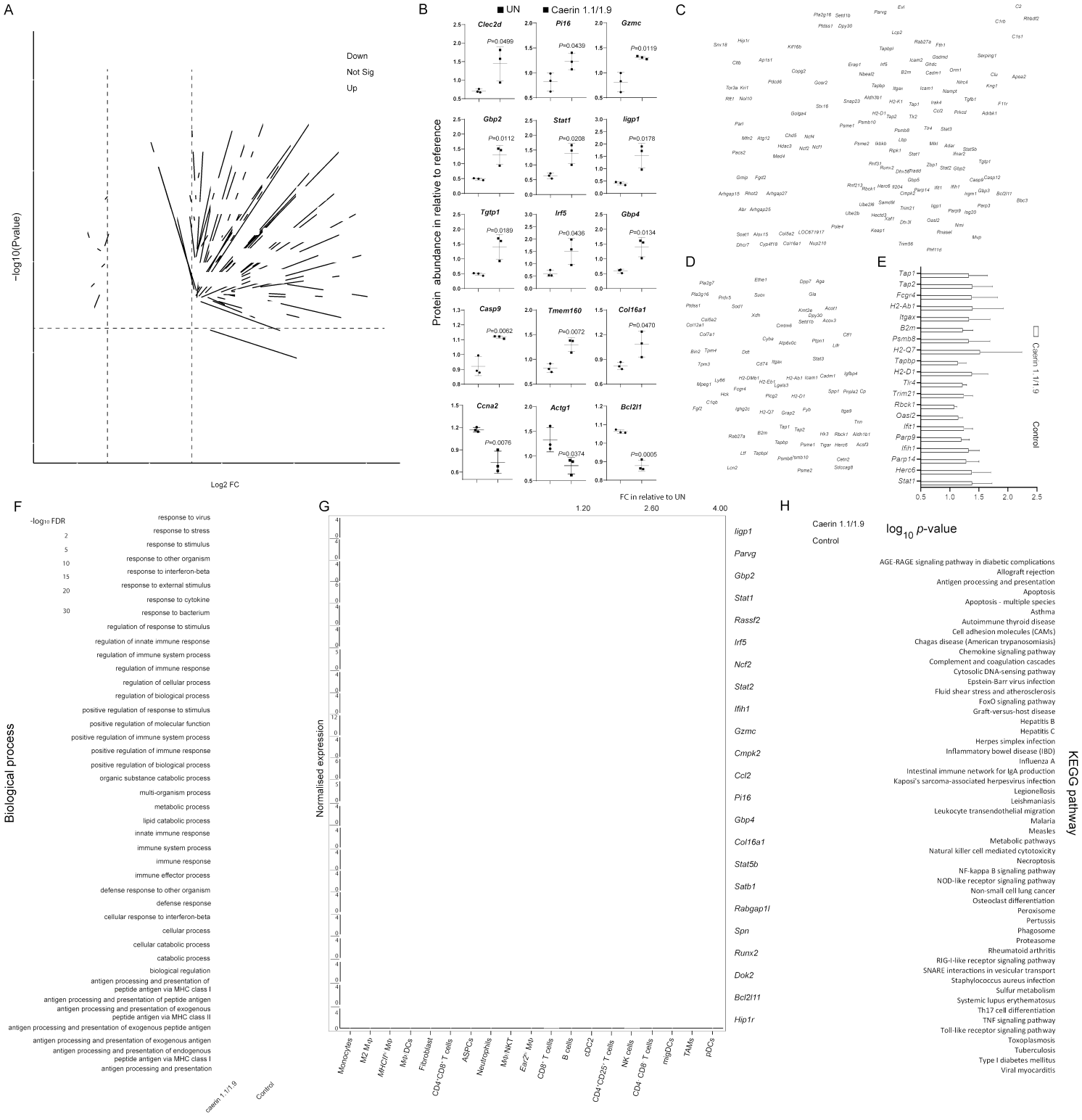

Figure 6

Quantitative proteomic analysis of TC-1 tumour in different groups (untreated, caerin 1.1/1.9 or P3). (A) The volcano graph shows proteins significantly regulated (FC>1.5, P<0.05) only in caerin 1.1/1.9 group with respect to untreated group. (B) Comparison of the abundance of selected proteins in untreated and caerin 1.1/1.9 groups in relative to reference. Two tailed student t test was used to evaluate the significance. PPIs of significantly upregulated proteins in caerin 1.1/1.9 group (C) and P3 group (D); the

size and the colour of the nodes represent the interaction degree of the protein. (E) Comparison of fold change (with respect to internal references) of the top 10 highest degree values on the PPIs in caerin 1.1/1.9 and P3 groups. (F) Comparison of biological processes enriched in the significantly elevated proteins in caerin 1.1/1.9 and P3 groups, respectively, with respect to untreated group. (G) The correlation between the gene expressions (in 19 cell populations) of the proteins showing significant upregulation only in caerin 1.1/1.9 group, and the fold change of these proteins in relative to untreated group. (H) The KEGG pathways enriched in caerin 1.1/1.9 and P3 groups ($P<0.05$).

Supplementary Files

This is a list of supplementary files associated with this preprint. Click to download.

- DescriptionofAdditionalSupplementaryFiles.docx
- Supplementaryfigures.docx
- SupplementaryFile1.pdf
- SupplementaryFile2.docx
- SupplementaryData1.xlsx
- SupplementaryData2.xlsx
- SupplementaryData3.xlsx
- SupplementaryData4.xlsx
- SupplementaryData5.xlsx
- SupplementaryData6.xlsx
- SupplementaryData7.xlsx